

Universidade Federal do Rio grande do Sul
Faculdade de Medicina - UFRGS
Pós - Graduação em Cardiologia e Ciências Cardiovasculares

Tese de Doutorado

Estudos do perfil de estresse oxidativo e mediadores de remodelamento ventricular em modelo experimental de infarto agudo do miocárdio e o papel do uso precoce de terapia celular

Angela Maria Vicente Tavares

Orientação: Profa. Dra. Nadine Clausell

Co-Orientação: Prof. Dr. Luis Eduardo P. Rohde

Porto Alegre – Dezembro de 2008.

SUMÁRIO

EPIGRAFE	03
AGRADECIMENTOS	04
RESUMO	07
INTRODUÇÃO	08
REFERÊNCIAS BIBLIOGRÁFICAS	22
JUSTIFICATIVAS	33
HIPOTESSES	34
OBJETIVO GERAL	35
Objetivos específicos (artigos 01 e 02)	35
ARTIGO 01	36
ARTIGO 02	51
CONCLUSÕES	70

*“ Não ande pelo caminho traçado;
Ele conduz somente até onde os outros já foram.”
A. Einstein*

*...“Não DIGAS nada!
Não, nem a verdade!
Há tanta suavidade
Em nada se dizer
E tudo se entender –
Tudo metade
De sentir e de ver...
Não digas nada!
Deixa esquecer.*

*Talvez que amanhã
Em outra paisagem
Digas que foi vã
Toda esta viagem
Até onde quis
Ser quem me agrada...
Mas ali fui feliz...
Não digas nada.”*

Fernando Pessoa

AGRADECIMENTOS

“A única coisa que não nos pode ser tomado é o conhecimento, mas a tarefa de obtê-lo não deve ter objetivo de passagem; ela deve servir a um propósito humano e este, causar felicidade a quem esteja buscando, pois é para isso que se vive. A busca de grandes ideais é um universo de pequenos gestos, portanto, retirar o melhor aprendizado da pior das situações, não é uma tarefa fácil, mas nos deixa mais fortes para a próxima etapa”. *Dissertação de Mestrado - A. Tavares, 2003.*

Tenho um único mérito em todo este trabalho, uma inexplicável capacidade de agregar e manter próximas pessoas competentes, comprometidas com os seus ideais de pesquisa e, o mais importante: que acreditaram nos meus objetivos e confiaram na minha miserável condição de começar um processo novo.

Tenho a exata noção de quanto este trabalho foi incapaz de demonstrar o enorme esforço de todos para que tivéssemos a oportunidade de contribuir com a ciência de forma inequívoca. Por isso, peço desculpas; fomos capazes de gerar tantos dados importantes, mas a incoerência das circunstâncias, às vezes, faz nosso tempo limitado e diminuto perante tudo o que gostaríamos e poderíamos mostrar.

Por fim, eu tive o privilégio de conviver, porque eu escolhi conviver, com seres humanos admiráveis, pesquisadores apaixonados, profissionais impressionantes e amigos muito especiais.

O Hospital de Clínicas foi minha casa por quatro anos, não tenho palavras para agradecer a oportunidade de ter estado aqui e o orgulho que sinto disso.

Uma pesquisadora por excelência, um ser humano e uma médica preocupada em levar o melhor aos seus pacientes; que saibam todos: esta foi e sempre será minha orientadora, Dra. Nadine Clausell; ser orientada por ela foi, sem dúvida, uma experiência única. Sob sua orientação se aprende ou se aprende... E se aprende!

Talvez esta seja a melhor tradução para “vai dar certo!” O que posso dizer é que simplesmente, mais que um privilégio, foi uma honra!

Agradeço ao Dr. Luis Eduardo Rohde, meu Co-Orientador por acreditar, muito mais do que eu, que realmente eu pudesse manusear uma ferramenta tão importante como é o Eco. Seu apoio para que eu pudesse utilizar o equipamento me deu a oportunidade de ajudar outros pesquisadores e participar de outros projetos, me tornando mais útil para todos.

Agradeço a toda a equipe que a compõe a Unidade de Experimentação Animal, pois foram incansáveis para facilitar o nosso trabalho com os animais, em todos os sentidos.

Um agradecimento especial a Profa. Roseli Moleck(†), veterinária chefe que nos deu todo o suporte para que pudéssemos iniciar o trabalho e nos acolheu com tanto carinho e empenho, sempre comprometida com tudo e com todos.

Agradeço as colegas do Laboratório de Pesquisa Cardiovascular pelo apoio e os momentos de alegria;

Aos meus colegas do LaFiEx, agradeço a oportunidade de poder participar das suas pesquisas e principalmente pelo voto de confiança.

Agradeço aos colegas da Terapia Gênica, onde me sinto em casa e tive apoio para realizar minha pesquisa, em especial ao Guilherme Baldo, sempre pronto a colaborar.

A Dra. Ursula Matte, um daqueles seres humanos admiráveis, pesquisadora apaixonada, profissional impressionante e amiga muito especial. Sentirei falta das descobertas inusitadas. As cartilagens que nos perdoem...

Aos meus bolsistas (Andréia Taffarel, Gabriela Nicolaidis e Rafael Dall’Alba) um agradecimento especial, pois foram muito mais do que alunos de iniciação científica; foram uma amostra de pesquisadores de futuro, profissionais competentes e pessoas

que vou lembrar sempre com carinho. A qualidade do trabalho passou pelas mãos deles e também por isso foi um trabalho de qualidade.

Dra. Adriane Belló-Klein também faz parte daqueles seres humanos admiráveis pesquisadores apaixonados, muito melhores do que eu, em quem, não só me espelhei como modelo de pesquisadora, mas que fez toda a diferença para que este doutorado pudesse ser concretizado. Parece mais o meu anjo da guarda, pois me acompanha desde o mestrado, sempre intervindo para que as coisas nunca dêem erradas para mim. Faz parte da minha família de amigos. Espero, um dia, poder retribuir.

Agradeço ao Laboratório de Fisiologia Cardiovascular como um todo, à Tânia, sempre pronta a ajudar com muita dedicação, aos colegas de Pós-graduação, extremamente prestativos e em especial ao Alex Sander, um dos melhores pesquisadores de bancada que já tive o privilégio de conhecer e conviver, um dos meus melhores amigos.

Agradeço a Dra. Maria Flávia que abriu seu laboratório para que eu pudesse terminar meus experimentos de Western blot.

Por fim, a minha família! Afinal, família são aquelas pessoas que a gente escolhe... As pessoas que me acolhem e que eu me dedico, um agradecimento especial: Maria, sempre uma inspiração de humanidade, competência e carinho ao tratar com as pessoas; Guega, Jaci e Denise, pessoas que me lembram sempre que mesmo longe, eu faço parte de alguma coisa; Lucia Longui, mesmo à distância nunca esquece de me manter por perto e Daniel Merel e Charles Knoblich... Lembram-me sempre, que aproveitar a vida é impressionantemente fácil, quando se sabe!

Vó Olívia, Vô Padão... Estes serão meus avós perfeitos pela eternidade, sempre que penso neles tenho certeza absoluta que o dia de amanhã será melhor... E fico em paz!

Resumo

A insuficiência cardíaca (IC) é uma síndrome clínica complexa com diversas etiologias e elevada prevalência. No infarto agudo do miocárdio, a oclusão aguda da artéria coronária resulta em alterações complexas da arquitetura ventricular. Estas alterações começam a se estabelecer imediatamente após a oclusão arterial, progredindo por várias semanas após o dano isquêmico inicial. O processo inflamatório e a liberação de citocinas fazem parte da resposta a injúria sofrida pelo tecido e desempenha um papel importante no período pós-infarto. Dentre os múltiplos fatores que contribuem para a progressão do remodelamento ventricular, a participação das espécies ativas de oxigênio (EAOs) neste processo é de extrema relevância. Diante deste quadro, novas estratégias terapêuticas têm sido propostas e a terapia celular surge como uma alternativa viável promissora objetivando, em última análise, o reparo cardíaco.

A hipótese inicial de que as células-tronco adultas poderiam ter efeito regenerativo do tecido miocárdio tem sido revisada e hoje, é cada vez mais aceito e reconhecido que as células-tronco adultas tem pouca ou nenhuma capacidade regenerativa e que os seus efeitos benéficos envolvam ações parácrinas sobre o tecido hospedeiro.

Neste estudo avaliamos o perfil oxidativo e sua correlação com o processo inflamatório e função cardíaca, precocemente, 48 horas pós-infarto agudo do miocárdio (IAM). Analisamos também estes mesmos parâmetros no tecido cardíaco de animais infartados que receberam tratamento com terapia celular.

Nosso estudo sugere que o comprometimento da função ventricular precocemente pós-IAM parece se associar com um desequilíbrio do estado redox e este por sua vez interage com os processos iniciais do fenótipo de remodelamento ventricular.

A terapia celular, com células derivadas da medula óssea num modelo experimental de 48 horas pós-IAM, foi associada com redução da hipertrofia ventricular e menor secreção de citocinas inflamatórias sugerindo ações parácrinas das células, nesta janela temporal.

INTRODUÇÃO

A insuficiência cardíaca (IC) é uma síndrome clínica complexa com diversas etiologias e elevada prevalência. Embora grandes avanços tenham ocorrido, consiste em uma preocupação crescente dos diferentes sistemas de saúde pública pelo seu elevado impacto econômico associado, particularmente, os custos das internações hospitalares. Este, e o seu prognóstico clínico sombrio, apesar de tratamentos otimizados, tem sido a tônica na busca de novas terapias.

Aspectos Epidemiológicos

As doenças cardiovasculares tornaram-se o principal problema de saúde em todo o mundo, ultrapassando o câncer e infecções como a principal causa de morte de muitos países em desenvolvimento^{1;2}. Embora a mortalidade por doença arterial coronariana tenha diminuído devido a avanços nos tratamentos de aterosclerose, hipercolesterolemia, hipertensão e diabetes³, as doenças cardiovasculares ainda representam 1 em cada 2,7 mortes nos Estados Unidos, traduzindo-se em aproximadamente 2,5 milhões de mortes todos os anos⁴. Além disso, a prevalência dos fatores de risco para doenças cardiovasculares, como hipertensão, diabetes tipo II e obesidade, tem aumentado nos últimos anos⁵⁻⁷.

Num estudo realizado em mais de 300 hospitais, nos Estados Unidos, foram rastreadas 2,5 milhões de internações, onde 496.534 pacientes (19,7%) tiveram IC, como desfecho primário ou secundário com uma média de permanência hospitalar de 8,7±28,6 dias e mortalidade intra-hospitalar de 7,1%. Neste estudo, as admissões de pacientes com IC como desfecho primário ou secundário foram associadas com pior prognóstico⁸.

No Brasil, de um total de 1.006.375 de mortes por qualquer causa, 6,4% foram por IAM, somente no ano de 2005. O número de internações hospitalares por IC foi de

293.473, cerca de 2,6% de todas as internações hospitalares por qualquer causa, ocorridas somente no ano de 2007⁹.

Remodelamento Ventricular Pós-Infarto Agudo do Miocárdio

Os estudos que descreveram pioneiramente o remodelamento ventricular (RV) na progressão da IC são aqueles utilizando como modelo o desenvolvimento de infarto agudo em ratos no início da década de 80 por Pfeffer e colaboradores¹⁰. Estes estudos demonstraram que a oclusão aguda da artéria coronária, particularmente quando ocorrem lesões transmuralis de grandes proporções, resulta em alterações complexas da arquitetura ventricular. Estas alterações começam a se estabelecer imediatamente após a oclusão arterial, progredindo por várias semanas após o dano isquêmico inicial¹¹.

Uma série de respostas compensatórias ocorre no ventrículo esquerdo após o IAM, com o objetivo primordial de preservar o débito cardíaco. A distensão aguda do tecido miocárdico viável e a ação do mecanismo de *Frank-Starling*, bem como o aumento da atividade cronotrópica e inotrópica secundária a estimulação simpática, buscam manter a função de bomba do ventrículo esquerdo, apesar da perda abrupta do tecido contrátil¹². A expansão da zona infartada ocorre poucas horas após o dano ao miocárdio, resultando em estresse e dilatação da parede ventricular¹³. A dilatação ventricular, embora represente um mecanismo eficiente de compensação, restabelecendo o volume sistólico, também tem sido consistentemente associada com uma diminuição de sobrevida¹⁴.

Embora grandes avanços tenham sido alcançados no entendimento dos mecanismos hemodinâmicos, histológicos e moleculares envolvidos nas alterações, que ocorrem no tecido cardíaco após um dano isquêmico, muitos pacientes que sofrem eventos agudos, mesmo tratados de forma otimizada, desenvolvem dilatação ventricular progressiva e podem evoluir para quadros clínicos de IC¹⁵.

Muito além de adaptações hemodinâmicas secundárias, eventos celulares e moleculares precoces pós-infarto, como a ativação de citocinas inflamatórias, estresse oxidativo, hipertrofia de miócitos, apoptose, necrose, fibrose e ativação proteolítica parecem exercer papéis centrais na progressão do RV¹⁶⁻¹⁹. Além de implicações mecânicas, estes eventos podem ser alvo de terapias mais objetivas e eficazes no combate a progressão da doença²⁰.

Papel da Modulação Inflamatória

O processo inflamatório e a liberação de citocinas fazem parte da resposta à injúria sofrida pelo tecido e desempenham um papel importante no período pós-infarto. A consequência dos efeitos das citocinas inflamatórias podem ser favoráveis, levando à cicatrização e restauração da função cardíaca, ou desfavoráveis levando, agudamente, ao um processo de dilatação e posteriormente, aos desfechos que culminam em IC²¹.

A modulação imunoinflamatória tem papel fundamental relacionada a fisiopatogenia da IC e sua correlação direta com o estresse oxidativo²². A indução da expressão gênica pelo fator nuclear kappa-beta (NFκ-B), envolvendo sinalização redox é um dos mecanismos moleculares que envolvem as sinalizações redox-sensíveis. O NFκ-B pode ser ativado por agentes oxidantes e inibido por agentes antioxidantes²³. A proteína NFκ-B se transloca para o núcleo, onde se liga ao gene alvo, ativando a transcrição de genes, cujos produtos atuam como mediadores pró-inflamatórios²⁴.

Citocinas pró-inflamatórias como interleucina 1 beta (IL-1β), fator de necrose tumoral alfa (TNF-α) e interleucina 6 (IL-6) não são constitutivamente expressas no tecido cardíaco normal²⁵. O aumento da produção destas citocinas representa uma resposta intrínseca ao estresse mecânico provocado pela injúria. Das primeiras horas até um dia pós-infarto estas citocinas tem sua expressão de mRNA aumentada na área infartada, assim como, em áreas não infartadas do miocárdio^{26;27}.

Estas citocinas inflamatórias são mediadores biológicos que têm sido encontradas em concentrações séricas elevadas em pacientes com IC²⁸. Em um estudo avaliando marcadores inflamatórios no momento do infarto comparados após um seguimento de oito anos mostrou que aqueles pacientes sobreviventes tinham os menores níveis séricos de IL-6 no momento do infarto²⁹.

Papel do Estresse Oxidativo

Dentre os múltiplos fatores que contribuem para a progressão do RV, vários estudos apontam para a participação de radicais livres e em especial as espécies ativas de oxigênio (EAOs) neste processo^{30;31}. Por exemplo, as EAOs tem sido referenciadas como fortemente implicadas na gênese da hipertrofia cardíaca³². A hipertrofia cardíaca pode ser tanto compensatória como adaptativa ou um indício de mal-adaptação, como um precursor da IC. Muitos dos fatores extracelulares que são capazes de induzir a hipertrofia dos cardiomiócitos e os fatores que medeiam esta podem ser ativados direta ou indiretamente pelas EAOs³³.

Estudos experimentais mostram diminuição da atividade antioxidante e aumento do estresse oxidativo, resultando no aumento da produção de radicais livres³⁴. Neste contexto, a contratilidade miocárdica pode estar deprimida em decorrência da redução de Ca^{++} proveniente do retículo sarcoplasmático e da atividade da Ca^{++} ATPase no tecido cardíaco³⁵. Outros estudos relacionam alterações morfológicas, como hipertrofia e apoptose dos cardiomiócitos, e disfunção da contratilidade miocárdica com o aumento da expressão das isoformas da NOS (óxido nítrico sintase): NOS endotelial (eNOS) e NOS induzida (iNOS)³⁶.

Devido a estas alterações metabólicas, é possível inferir que as conseqüentes modificações nos processos de oxi-redução que ocorrem na célula, e conseqüentemente no “status” de estresse oxidativo ao qual este órgão está submetido, são também responsáveis diretos pelo processo de RV e pelos fenótipos apoptóticos^{37;38}.

Durante a fase de inflamação aguda pós-IAM, neutrófilos e monócitos produzem mieloperoxidases (MPO) que, apesar de constituírem uma das primeiras linhas de defesa do sistema imunitário inato, induzem a formação de EAOs e subseqüentemente contribuem para o processo de remodelamento do miocárdio³⁹. Clinicamente, altos níveis plasmáticos de MPO predizem aumento de mortalidade de pacientes que sofreram IAM⁴⁰.

Em um estudo utilizando MPO marcada com quelato de gadolínio e análise por ressonância magnética, foi demonstrado que o uso de atorvastatina em camundongos infartados diminuía de forma significativa a expressão dessa enzima já em 48 horas pós-infarto. O grupo controle também demonstrou que o maior pico de MPO se deu nas mesmas 48 horas demonstrando que as alterações bioquímicas no RV associadas a estresse oxidativo ocorrem muito precocemente após o infarto⁴¹.

Evidências de estudos clínicos na IC, apontam para a importância dos processos de oxi-redução. Através de estudos envolvendo lipoperoxidação (LPO) e atividade antioxidante (GPx e vitamina C) de pacientes com diferentes graus de IC congestiva, foi encontrado um progressivo aumento de danos induzidos por radicais livres e diminuição das reservas antioxidantes diretamente proporcionais ao grau da IC⁴².

A busca de intervenções que reduzam o dano oxidativo justifica algumas iniciativas clinico-experimentais. Por exemplo, em pacientes portadores de cardiopatia isquêmica ou com cardiomiopatia dilatada, a atividade de NADPH-oxidase está elevada e foi associada ao aumento da atividade GTPase rac-1. O uso de estatinas nestes pacientes diminuiu a atividade da rac-1 no miocárdio, possivelmente demonstrando o efeito destas drogas sobre a atividade das EAOs⁴³. O tratamento com alopurinol, um inibidor da XO (xantina-oxidase), enzima que induz a formação de EAOs, melhora a contratilidade do miocárdio e restaura a reatividade vasomotora^{44;45}. Por fim, o probucol, droga com função redutora de colesterol e importantes propriedades antioxidantes, foi capaz de diminuir a expressão gênica de IL-6 e o estresse oxidativo, 24 horas após o infarto⁴⁶.

Terapia celular

As terapias biológicas estão cada vez mais presentes trazendo expectativas de renovação na área de saúde com perspectivas terapêuticas melhores nas diversas áreas do conhecimento.

As células-tronco (*stem cells*) se diferenciam das outras células do organismo por apresentarem três características: a) são indiferenciadas e não especializadas; b) tem um potencial de replicação sem a necessidade de diferenciar-se, de tal forma que um pequeno número de células pode gerar uma maior população de células semelhantes; c) também são capazes de diferenciar-se em células especializadas de um tecido específico⁴⁷⁻⁴⁹.

Tipos de células candidatas a uso em terapia celular

Fonte	Vantagem	Desvantagem
Cardiomiócito Fetal;	Fenótipo de cardiomiócito;	Imunossupressão; debate ético; curta sobrevida e limitada disponibilidade;
Mioblásto Esquelético	Sem Imunogenicidade, autó- logo; fadiga e isquemia resistente e disponível;	Arritmias, sem “gap”
C. Progenitoras Endoteliais;	sem rejeição; autóloga;	Necessita Expansão;
C. Tronco Embrionárias	Pluripotente, altamente expansível;	Imunossupressão; debate ético; dispo- nibilidade, tumor?
C. Tronco Mesenquimais adultas	Sem rejeição, autólogo, Pluripotente, criopreservável;	Propriedade funcional e não esclarecida; dificuldade para isolar em cultura;

Tabela – *Tipos de células utilizadas em pesquisas pré-clínicas e/ou clínicas – vantagens e desvantagens observadas no uso destas células in vivo*⁵⁰;

Um exemplo de regeneração de tecido são as células que compõem o músculo esquelético, onde células satélites (mioblastos esqueléticos) armazenadas entre as lâminas basais e as fibras musculares têm papel importante de regeneração, pois são

células quiescentes à espera de um estímulo de resposta a uma injúria que as possibilitará se diferenciarem em miócitos maduros, com o objetivo de reparar a área lesada⁵¹.

De acordo com a sua origem, as células podem ser classificadas como: células-tronco embrionárias e adultas ou somáticas.

Células-tronco Embrionárias

Células-tronco embrionárias são isoladas e retiradas de blastocistos embrionários capazes de proliferar e se diferenciar em células das três linhagens germinativas diferentes em células de qualquer tecido. Também são capazes de se proliferarem indefinidamente, mantendo sua capacidade de diferenciação, resultando, assim, em uma fonte potencialmente ilimitada^{52;53}.

Células-tronco embrionárias são consideradas as mais versáteis, podendo dar origem a diversos tipos celulares incluindo cardiomiócitos⁵⁴. Em estudos experimentais, realizados em animais, foi observada uma grande capacidade proliferativa das células-tronco embrionárias. Uma vez implantadas diretamente no miocárdio foram responsáveis pela diminuição da área de infarto com melhora da função cardíaca e acoplamento elétrico observado pela detecção da expressão da proteína conexina 43⁵⁵.

Apesar dos benefícios mostrados com o uso destas células, não é possível descartar a possibilidade de formação de teratomas e tumores (Figura 1)⁵⁶.

Desenvolvimento das Células-Tronco Embrionárias

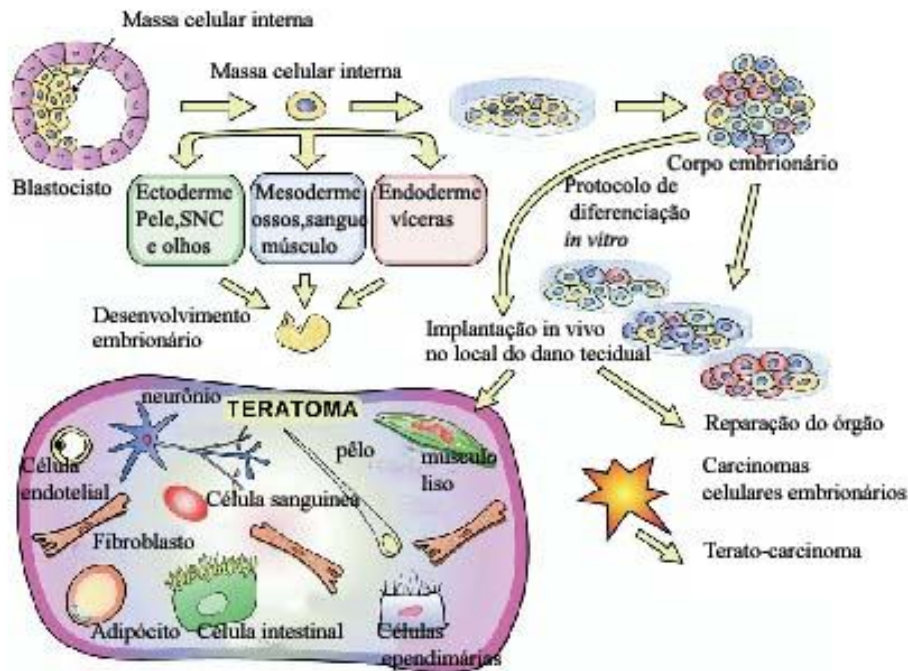


Figura 1 - Células-tronco embrionárias. Durante o desenvolvimento, as células-tronco embrionárias (CES) dão origem a ectoderme, mesoderme e endoderme. CES são obtidas a partir da massa celular interna do blastocisto e *in vitro* forma organismos embriões (EBS) que contêm células indiferenciadas (amarelo), ectodérmicas (verde), mesodérmicas (azul), e endodérmicas (vermelho). A implantação da EBS, *in vivo*, pode reparar órgãos danificados e gerar tumores⁵⁷.

Células-tronco adultas ou somáticas

As células-tronco adultas comportam, pelo menos, três diferentes grupos: 1) células-tronco derivadas da medula óssea; 2) células-tronco circulantes ou células progenitoras que também, pelo menos em parte, são derivadas a partir da medula óssea e 3) células-tronco residentes do tecido. A medula óssea contém uma complexa variedade de células progenitoras, incluindo as células-tronco hematopoiéticas (HSCs), as células-tronco mesenquimais (CTMs) ou células estromais, e as células progenitoras adultas (MAPCs), um subgrupo das células CTMs⁵⁸.

Outra população de células progenitoras a mostrar um potencial terapêutico foram encontradas no sangue circulante, são as chamadas células progenitoras endoteliais

(EPCs), definidas pela sua capacidade de formar novos vasos sanguíneos pós-isquemia⁵⁹.

As células-tronco de medula óssea são, basicamente, responsáveis por manter a homeostase dos tecidos, substituindo células que foram perdidas na maturação, no envelhecimento ou por qualquer tipo de injúria que o tecido tenha sofrido. A partir de um processo fisiológico, elas são capazes de migrar até o tecido alvo, através do sangue periférico, bem como, retornar novamente para a medula⁶⁰.

Estas células, cujo potencial parece ilimitado, têm se mostrado como candidatas ideais, já bastante utilizadas no tratamento de doenças hematológicas.

Terapia Celular e Cardiopatias

Um dos motivos pelo qual a terapia celular tem sido amplamente estudada objetivando reparo cardíaco, é o fato de haver um conceito de uma relativa incapacidade das células-tronco residentes na medula óssea em migrar para o miocárdio lesado ou quando no miocárdio, se auto-regenerar.^{61;62} Entretanto, a definição do coração como um órgão de diferenciação terminal, foi contestada pela observação de células cardíacas precoces em um estado mitótico. De fato, Beltrami e colaboradores analisaram a proliferação de cardiomiócitos em pacientes que foram a óbito entre 4 e 12 dias pós-infarto e observaram células em mitose na zona adjacente ao infarto, bem como, em zonas distantes da área de lesão⁶³.

Atualmente, diversos tipos de regeneração de celular estão sendo investigados, bem como vários tipos de células que possam demonstrar alguma capacidade de proliferar e se diferenciar em cardiomiócitos funcionais^{64;65}.

Em 2004, pesquisadores procuraram reproduzir os experimentos de Orlic e colaboradores de transdiferenciação de células de medula óssea para o reparo do tecido cardíaco lesado⁶⁶. Os resultados não foram concordantes com os experimentos

anteriores, pois as células implantadas não expressaram marcadores específicos do tecido cardíaco. Além disso, estas células adotaram seu tradicional destino hematopoiético^{67;68}.

Experimentalmente, em um estudo utilizando uma sub-população de células Lin⁻ckit⁺, isoladas a partir de corações de ratas adultas, *in vitro* e também *in vivo*, exibiram propriedades de células-tronco cardíacas. As células apresentaram capacidade de auto-renovação, sendo clonáveis e multipotentes e que puderam se diferenciar não somente em cardiomiócitos, mas também em células endoteliais e músculo liso. Embora estas células não apresentassem contração espontânea em cultivo, ao serem implantadas no miocárdio infartado melhoraram a função cardíaca mostrando que o miocárdio possui células-tronco residentes com capacidade regenerativa quando estimuladas⁶⁹

Os mioblastos esqueléticos, ou células satélites são células progenitoras que normalmente permanecem em um estado quiescente, são capazes de serem cultivadas *in vitro*, e se diferenciar conservando propriedades do músculo esquelético quando transplantadas em regiões infartadas⁷⁰.

Num estudo clínico realizado em cinco pacientes com cardiomiopatia isquêmica e listados para transplante cardíaco, que receberam o transplante de mioblastos esqueléticos, houve diferenciação das células musculares esqueléticas em fibras musculares maduras e um pequeno aumento na formação de vasos em três pacientes⁷¹.

O transplante celular utilizando mioblastos no coração, também conhecido como cardioplastia celular tem sido estudado como uma alternativa terapêutica para cardiopatias isquêmicas e não isquêmicas⁷². Como terapia para o tratamento do infarto, a cardioplastia celular tem como objetivo repovoar a cicatriz necrótica e as zonas adjacentes ao infarto com células potencialmente contráteis, capazes de substituir os cardiomiócitos mortos, restaurando a função das áreas acinéticas⁷³.

Por fim, há na literatura intenso interesse em avaliar desfechos clínicos com o uso de transplante autólogo de células-tronco de medula óssea. Alguns são exemplos clássicos de algumas estratégias utilizadas^{74;75}. O TOPCARE-AMI (*Transplantation of progenitor cells and regeneration enhancement in acute myocardial infarction*), um estudo de fase I incluiu 54 pacientes com IAM tratados com *stent* intracoronário que tiveram um seguimento de quatro meses enquanto trinta e sete foram avaliados após um seguimento de doze meses. Os pacientes receberam infusão intracoronária de células de medula óssea vinte e quatro horas após o IAM. Os grupos foram divididos por tempo de seguimento. Houve um aumento na fração de ejeção de $50\pm 10\%$, antes do procedimento, para $58,3\pm 10\%$ ($p < 0.001$). Uma limitação deste estudo foi a falta de um grupo controle. Foi demonstrado com isso, apenas a viabilidade e a segurança deste tipo de procedimento^{76;77}.

Num estudo observacional realizado em dez pacientes com histórico de IAM e fração de ejeção $< 35\%$, foram administrados mioblástos esqueléticos por via intramiocárdica. Após um seguimento de dez meses foi observado um aumento da fração de ejeção de 23% para 32% ($p < 0.03$) e uma melhora do encurtamento funcional. Apesar destes resultados, a classe funcional passou de $2,7$, antes do transplante, para $1,6$, após o tratamento. Além disso, quatro pacientes apresentaram taquicardia ventricular sustentada e foi necessário o implante de um cardio-desfibrilador⁷⁸.

Em outro estudo, de fase II, foi utilizado um estimulador de mobilização de células-tronco, a partir de sangue periférico (*Granulocyte-colony-stimulating factor*) G-CSF, infundido por infusão intracoronária. Foram arrolados 27 pacientes com IAM que receberam *stent* coronário. Após seis meses de seguimento, o grupo de pacientes, que recebeu terapia celular, obteve melhora da fração de ejeção de $48,7\pm 8,3\%$, antes do tratamento, para $55,1\pm 7,4\%$ ($p < 0.005$), após os seis meses de seguimento. Um resultado

inesperado deste estudo foi a alta taxa de reestenose nos pacientes que receberam o tratamento com terapia celular⁷⁹.

O estudo BOOST (*Bone Marrow Transfer to Enhance ST-Elevation Infarct Regeneration*) foi conduzido com objetivo de avaliar o efeito da transferência de autóloga intracoronária de células da medula óssea sobre a fração de ejeção. Foi um estudo controlado, randomizado que envolveu 60 pacientes que haviam sofrido infarto agudo com elevação ST sustentada submetidos à reperfusão coronária percutânea. A fração de ejeção global avaliada por ressonância magnética foi significativamente aumentada nos pacientes tratados com transplante de medula óssea de $50 \pm 10\%$ antes do tratamento para $56.7 \pm 12.5\%$ versus controles, $51.3 \pm 9.3\%$ para $52.0 \pm 12.4\%$, avaliados após seis meses de seguimento ($P=0.0026$). Apesar dos resultados revelarem melhora na função sistólica em seis meses, este aumento da fração de ejeção global não foi sustentado até 18 meses de seguimento destes pacientes. O estudo mostrou uma melhora na função cardíaca, com pouca viabilidade, a longo prazo, não se traduzindo em permanente reparação do miocárdio⁸⁰.

O uso de terapia celular merece ainda algumas considerações críticas da sua aplicabilidade e segurança. Uma das limitações do uso das células-tronco de medula óssea é a possibilidade de que estas possam diferenciar-se em outros tipos celulares, como os fibroblastos, ao serem implantadas em uma zona onde esteja se desenvolvendo uma cicatriz fibrótica⁸¹, contribuindo para o risco de eventuais arritmias ventriculares. Neste sentido, a utilização mais precoce destas células parece ser uma alternativa mais atraente nos tratamentos com terapia celular⁵⁶.

Embora estas informações sejam pouco encorajadoras, abre-se a possibilidade de que estas células tenham um papel muito mais complexo, de ação parácrina, junto ao tecido cardíaco lesado e, outras abordagens devam ser avaliadas como respostas importantes no entendimento dos efeitos da terapia celular⁸².

Segundo Menasché, a hipótese inicial de que as células-tronco adultas poderiam ter efeito regenerativo do tecido miocárdio levou a um habitual enfoque na fração de ejeção como o principal parâmetro a ser analisado. Hoje, é cada vez mais aceito e reconhecido que as células-tronco adultas, em contraste com as células embrionárias tem pouca ou nenhuma capacidade regenerativa e que os seus efeitos benéficos envolvam ações parácrinas sobre o tecido hospedeiro⁸².

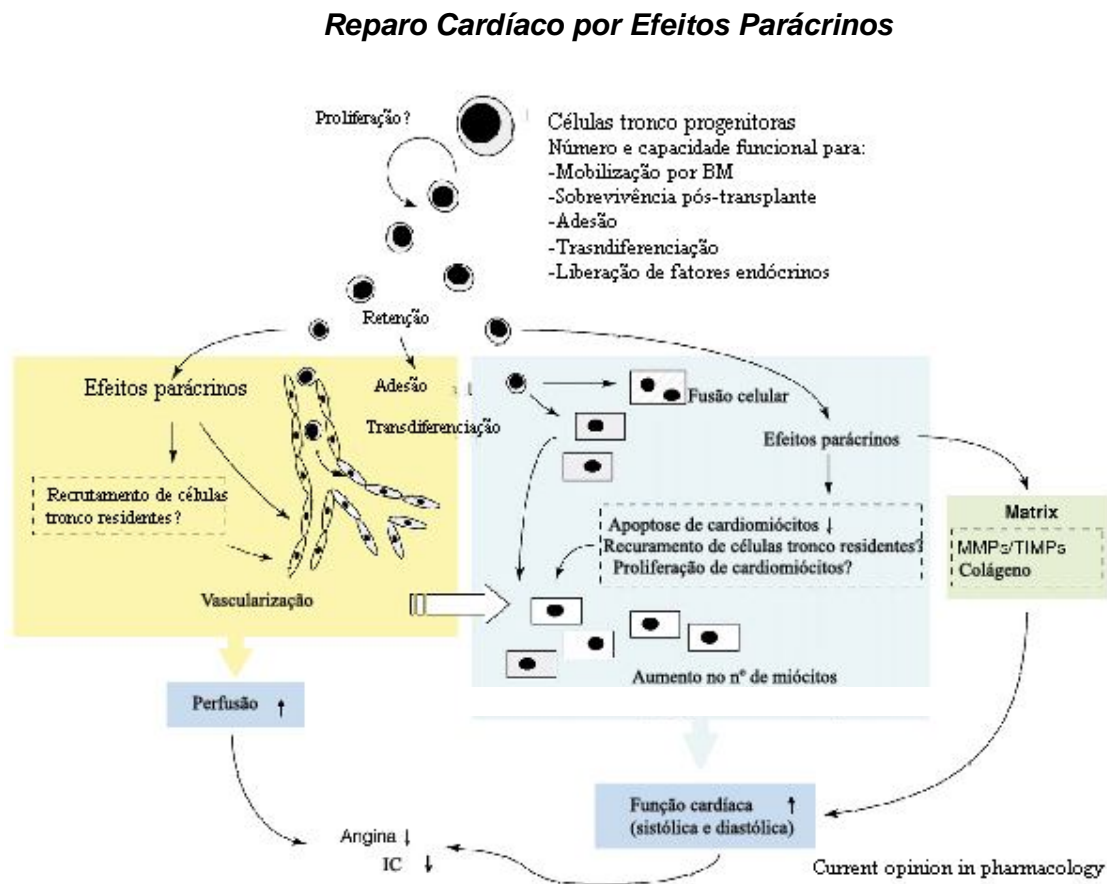


Figura 2 - O transplante de células progenitoras pode ter um impacto favorável no desempenho contrátil e perfusão tecidual, promovendo a vascularização e formação de miócitos. Dependendo do tipo, local e meio de administração das células-tronco, sua contribuição relativa na incorporação (transdiferenciação e/ou fusão) versus efeitos parácrinos podem variar. O número de células progenitoras e sua capacidade funcional são diretamente influenciadas pela idade, sexo, fatores de risco cardiovasculares e doenças subjacentes⁸³.

Em suma, parece claro que houve uma migração talvez um pouco precoce para estudos clínicos com terapia celular em cardiopatias, ainda sem que houvesse um mais

completo e abrangente entendimento dos diversos mecanismos envolvidos nos seus efeitos benéficos e além de explorar potenciais efeitos indesejáveis associados, que poderiam surgir ao longo do tempo.

Os estudos experimentais que compõem este documento procuram dissecar com maior detalhamento aspectos de estresse oxidativo, processo inflamatório e morte celular muito precocemente pós-IAM e estudar o efeito do uso de terapia celular nestes processos e sua repercussão em parâmetros ecocardiográficos.

Referências

1. Legrand C. Fifty-third World Health Assembly: impact on cardiovascular disease. *Can J Cardiol.* 2000;16:857-859.
2. Thom T, Haase N, Rosamond W, Howard VJ, Rumsfeld J, Manolio T, Zheng ZJ, Flegal K, O'Donnell C, Kittner S, Lloyd-Jones D, Goff DC, Jr., Hong Y, Adams R, Friday G, Furie K, Gorelick P, Kissela B, Marler J, Meigs J, Roger V, Sidney S, Sorlie P, Steinberger J, Wasserthiel-Smoller S, Wilson M, Wolf P. Heart disease and stroke statistics--2006 update: a report from the American Heart Association Statistics Committee and Stroke Statistics Subcommittee. *Circulation.* 2006;113:e85-151.
3. Smith SC, Jr., Allen J, Blair SN, Bonow RO, Brass LM, Fonarow GC, Grundy SM, Hiratzka L, Jones D, Krumholz HM, Mosca L, Pasternak RC, Pearson T, Pfeffer MA, Taubert KA. AHA/ACC guidelines for secondary prevention for patients with coronary and other atherosclerotic vascular disease: 2006 update: endorsed by the National Heart, Lung, and Blood Institute. *Circulation.* 2006;113:2363-2372.
4. Thom T, Haase N, Rosamond W, Howard VJ, Rumsfeld J, Manolio T, Zheng ZJ, Flegal K, O'Donnell C, Kittner S, Lloyd-Jones D, Goff DC, Jr., Hong Y, Adams R, Friday G, Furie K, Gorelick P, Kissela B, Marler J, Meigs J, Roger V, Sidney S, Sorlie P, Steinberger J, Wasserthiel-Smoller S, Wilson M, Wolf P. Heart disease and stroke statistics--2006 update: a report from the American Heart Association Statistics Committee and Stroke Statistics Subcommittee. *Circulation.* 2006;113:e85-151.
5. Appel LJ, Brands MW, Daniels SR, Karanja N, Elmer PJ, Sacks FM. Dietary approaches to prevent and treat hypertension: a scientific statement from the American Heart Association. *Hypertension.* 2006;47:296-308.

6. Haffner SM. Can reducing peaks prevent type 2 diabetes: implication from recent diabetes prevention trials. *Int J Clin Pract Suppl.* 2002;33-39.
7. Wyatt SB, Winters KP, Dubbert PM. Overweight and obesity: prevalence, consequences, and causes of a growing public health problem. *Am J Med Sci.* 2006;331:166-174.
8. Ng TM, Dasta JF, Durtschi AJ, McLaughlin TP, Feldman DS. Characteristics, drug therapy, and outcomes from a database of 500,000 hospitalized patients with a discharge diagnosis of heart failure. *Congest Heart Fail.* 2008;14:202-210.
9. DATASUS - Ministry of Health - Database available online at: www.datasus.gov.br, accessed Dec 01, 2008.
10. Pfeffer MA, Pfeffer JM, Fishbein MC, Fletcher PJ, Spadaro J, Kloner RA, Braunwald E. Myocardial infarct size and ventricular function in rats. *Circ Res.* 1979;44:503-512.
11. Pfeffer MA, Braunwald E. Ventricular remodeling after myocardial infarction. Experimental observations and clinical implications. *Circulation.* 1990;81:1161-1172.
12. Yousef ZR, Redwood SR, Marber MS. Postinfarction left ventricular remodeling: where are the theories and trials leading us? *Heart.* 2000;83:76-80.
13. Sutton MG, Sharpe N. Left ventricular remodeling after myocardial infarction: pathophysiology and therapy. *Circulation.* 2000;101:2981-2988.
14. White HD, Norris RM, Brown MA, Brandt PW, Whitlock RM, Wild CJ. Left ventricular end-systolic volume as the major determinant of survival after recovery from myocardial infarction. *Circulation.* 1987;76:44-51.

15. Rumberger JA, Behrenbeck T, Breen JR, Reed JE, Gersh BJ. Nonparallel changes in global left ventricular chamber volume and muscle mass during the first year after transmural myocardial infarction in humans. *J Am Coll Cardiol*. 1993;21:673-682.
16. Anversa P. Myocyte death in the pathological heart. *Circ Res*. 2000;86:121-124.
17. Nadal-Ginard B, Kajstura J, Leri A, Anversa P. Myocyte death, growth, and regeneration in cardiac hypertrophy and failure. *Circ Res*. 2003;92:139-150.
18. Pfeffer MA, Braunwald E. Ventricular remodeling after myocardial infarction. Experimental observations and clinical implications. *Circulation*. 1990;81:1161-1172.
19. Sutton MG, Sharpe N. Left ventricular remodeling after myocardial infarction: pathophysiology and therapy. *Circulation*. 2000;101:2981-2988.
20. Prabhu SD. Post-infarction ventricular remodeling: an array of molecular events. *J Mol Cell Cardiol*. 2005;38:547-550.
21. Nian M, Lee P, Khaper N, Liu P. Inflammatory cytokines and postmyocardial infarction remodeling. *Circ Res*. 2004;94:1543-1553.
22. Kaur K, Sharma AK, Dhingra S, Singal PK. Interplay of TNF-alpha and IL-10 in regulating oxidative stress in isolated adult cardiac myocytes. *J Mol Cell Cardiol*. 2006;41:1023-1030.
23. Haddad JJ. Oxygen homeostasis, thiol equilibrium and redox regulation of signalling transcription factors in the alveolar epithelium. *Cell Signal*. 2002;14:799-810.
24. Haddad JJ. Antioxidant and prooxidant mechanisms in the regulation of redox(y)-sensitive transcription factors. *Cell Signal*. 2002;14:879-897.

25. Kapadia SR, Oral H, Lee J, Nakano M, Taffet GE, Mann DL. Hemodynamic regulation of tumor necrosis factor-alpha gene and protein expression in adult feline myocardium. *Circ Res*. 1997;81:187-195.
26. Deten A, Volz HC, Briest W, Zimmer HG. Cardiac cytokine expression is upregulated in the acute phase after myocardial infarction. Experimental studies in rats. *Cardiovasc Res*. 2002;55:329-340.
27. Irwin MW, Mak S, Mann DL, Qu R, Penninger JM, Yan A, Dawood F, Wen WH, Shou Z, Liu P. Tissue expression and immunolocalization of tumor necrosis factor-alpha in postinfarction dysfunctional myocardium. *Circulation*. 1999;99:1492-1498.
28. Nian M, Lee P, Khaper N, Liu P. Inflammatory cytokines and postmyocardial infarction remodeling. *Circ Res*. 2004;94:1543-1553.
29. Jaremo P, Nilsson O. Interleukin-6 and neutrophils are associated with long-term survival after acute myocardial infarction. *Eur J Intern Med*. 2008;19:330-333.
30. Singal PK, Khaper N, Palace V, Kumar D. The role of oxidative stress in the genesis of heart disease. *Cardiovasc Res*. 1998;40:426-432.
31. Darley-Usmar V, Halliwell B. Blood radicals: reactive nitrogen species, reactive oxygen species, transition metal ions, and the vascular system. *Pharm Res*. 1996;13:649-662.
32. Kwon SH, Pimentel DR, Remondino A, Sawyer DB, Colucci WS. H₂O₂ regulates cardiac myocyte phenotype via concentration-dependent activation of distinct kinase pathways. *J Mol Cell Cardiol*. 2003;35:615-621.
33. Higuchi Y, Otsu K, Nishida K, Hirotani S, Nakayama H, Yamaguchi O, Matsumura Y, Ueno H, Tada M, Hori M. Involvement of reactive oxygen species-mediated NF-

- kappa B activation in TNF-alpha-induced cardiomyocyte hypertrophy. *J Mol Cell Cardiol.* 2002;34:233-240.
34. Singal PK, Khaper N, Farahmand F, Bello-Klein A. Oxidative stress in congestive heart failure. *Curr Cardiol Rep.* 2000;2:206-211.
 35. Chandra M, Surendra K, Kapoor RK, Ghatak A, Kaur G, Pandey NR, Misra MK. Oxidant stress mechanisms in heart failure. *Boll Chim Farm.* 2000;139:149-152.
 36. Stein B, Eschenhagen T, Rudiger J, Scholz H, Forstermann U, Gath I. Increased expression of constitutive nitric oxide synthase III, but not inducible nitric oxide synthase II, in human heart failure. *J Am Coll Cardiol.* 1998;32:1179-1186.
 37. Antozzi C, Zeviani M. Cardiomyopathies in disorders of oxidative metabolism. *Cardiovasc Res.* 1997;35:184-199.
 38. Pimentel DR, Amin JK, Xiao L, Miller T, Viereck J, Oliver-Krasinski J, Baliga R, Wang J, Siwik DA, Singh K, Pagano P, Colucci WS, Sawyer DB. Reactive oxygen species mediate amplitude-dependent hypertrophic and apoptotic responses to mechanical stretch in cardiac myocytes. *Circ Res.* 2001;89:453-460.
 39. Nahrendorf M, Swirski FK, Aikawa E, Stangenberg L, Wurdinger T, Figueiredo JL, Libby P, Weissleder R, Pittet MJ. The healing myocardium sequentially mobilizes two monocyte subsets with divergent and complementary functions. *J Exp Med.* 2007;204:3037-3047.
 40. Heinecke JW. Mechanisms of oxidative damage by myeloperoxidase in atherosclerosis and other inflammatory disorders. *J Lab Clin Med.* 1999;133:321-325.
 41. Nahrendorf M, Sosnovik D, Chen JW, Panizzi P, Figueiredo JL, Aikawa E, Libby P, Swirski FK, Weissleder R. Activatable magnetic resonance imaging agent reports

- myeloperoxidase activity in healing infarcts and noninvasively detects the antiinflammatory effects of atorvastatin on ischemia-reperfusion injury. *Circulation*. 2008;117:1153-1160.
42. Keith M, Geranmayegan A, Sole MJ, Kurian R, Robinson A, Omran AS, Jeejeebhoy KN. Increased oxidative stress in patients with congestive heart failure. *J Am Coll Cardiol*. 1998;31:1352-1356.
43. Maack C, Kartes T, Kilter H, Schafers HJ, Nickenig G, Bohm M, Laufs U. Oxygen free radical release in human failing myocardium is associated with increased activity of rac1-GTPase and represents a target for statin treatment. *Circulation*. 2003;108:1567-1574.
44. Cappola TP, Kass DA, Nelson GS, Berger RD, Rosas GO, Kobeissi ZA, Marban E, Hare JM. Allopurinol improves myocardial efficiency in patients with idiopathic dilated cardiomyopathy. *Circulation*. 2001;104:2407-2411.
45. Doehner W, Schoene N, Rauchhaus M, Leyva-Leon F, Pavitt DV, Reaveley DA, Schuler G, Coats AJ, Anker SD, Hambrecht R. Effects of xanthine oxidase inhibition with allopurinol on endothelial function and peripheral blood flow in hyperuricemic patients with chronic heart failure: results from 2 placebo-controlled studies. *Circulation*. 2002;105:2619-2624.
46. Sia YT, Parker TG, Liu P, Tsoporis JN, Adam A, Rouleau JL. Improved post-myocardial infarction survival with probucol in rats: effects on left ventricular function, morphology, cardiac oxidative stress and cytokine expression. *J Am Coll Cardiol*. 2002;39:148-156.
47. Verfaillie CM. Adult stem cells: assessing the case for pluripotency. *Trends Cell Biol*. 2002;12:502-508.

48. Orkin SH, Zon LI. Hematopoiesis and stem cells: plasticity versus developmental heterogeneity. *Nat Immunol.* 2002;3:323-328.
49. Anderson DJ, Gage FH, Weissman IL. Can stem cells cross lineage boundaries? *Nat Med.* 2001;7:393-395.
50. Lee MS, Makkar RR. Stem-cell transplantation in myocardial infarction: a status report. *Ann Intern Med.* 2004;140:729-737.
51. MAURO A. Satellite cell of skeletal muscle fibers. *J Biophys Biochem Cytol.* 1961;9:493-495.
52. Weissberg PL, Qasim A. Stem cell therapy for myocardial repair. *Heart.* 2005;91:696-702.
53. Leri A, Kajstura J, Nadal-Ginard B, Anversa P. Some like it plastic. *Circ Res.* 2004;94:132-134.
54. Maltsev VA, Rohwedel J, Hescheler J, Wobus AM. Embryonic stem cells differentiate in vitro into cardiomyocytes representing sinusnodal, atrial and ventricular cell types. *Mech Dev.* 1993;44:41-50.
55. Min JY, Yang Y, Converso KL, Liu L, Huang Q, Morgan JP, Xiao YF. Transplantation of embryonic stem cells improves cardiac function in postinfarcted rats. *J Appl Physiol.* 2002;92:288-296.
56. Lee MS, Lill M, Makkar RR. Stem cell transplantation in myocardial infarction. *Rev Cardiovasc Med.* 2004;5:82-98.
57. Leri A, Kajstura J, Anversa P, Frishman WH. Myocardial regeneration and stem cell repair. *Curr Probl Cardiol.* 2008;33:91-153.

58. Burchfield JS, Dimmeler S. Role of paracrine factors in stem and progenitor cell mediated cardiac repair and tissue fibrosis. *Fibrogenesis Tissue Repair*. 2008;1:4.
59. Urbich C, Dimmeler S. Endothelial progenitor cells: characterization and role in vascular biology. *Circ Res*. 2004;95:343-353.
60. Wright DE, Wagers AJ, Gulati AP, Johnson FL, Weissman IL. Physiological migration of hematopoietic stem and progenitor cells. *Science*. 2001;294:1933-1936.
61. Orlic D, Hill JM, Arai AE. Stem cells for myocardial regeneration. *Circ Res*. 2002;91:1092-1102.
62. Orlic D. The strength of plasticity: stem cells for cardiac repair. *Int J Cardiol*. 2004;95 Suppl 1:S16-S19.
63. Beltrami AP, Urbanek K, Kajstura J, Yan SM, Finato N, Bussani R, Nadal-Ginard B, Silvestri F, Leri A, Beltrami CA, Anversa P. Evidence that human cardiac myocytes divide after myocardial infarction. *N Engl J Med*. 2001;344:1750-1757.
64. Orlic D, Kajstura J, Chimenti S, Jakoniuk I, Anderson SM, Li B, Pickel J, McKay R, Nadal-Ginard B, Bodine DM, Leri A, Anversa P. Bone marrow cells regenerate infarcted myocardium. *Nature*. 2001;410:701-705.
65. Niagara MI, Haider HK, Jiang S, Ashraf M. Pharmacologically preconditioned skeletal myoblasts are resistant to oxidative stress and promote angiomyogenesis via release of paracrine factors in the infarcted heart. *Circ Res*. 2007;100:545-555.
66. Orlic D, Kajstura J, Chimenti S, Jakoniuk I, Anderson SM, Li B, Pickel J, McKay R, Nadal-Ginard B, Bodine DM, Leri A, Anversa P. Bone marrow cells regenerate infarcted myocardium. *Nature*. 2001;410:701-705.

67. Murry CE, Soonpaa MH, Reinecke H, Nakajima H, Nakajima HO, Rubart M, Pasumarthi KB, Virag JI, Bartelmez SH, Poppa V, Bradford G, Dowell JD, Williams DA, Field LJ. Haematopoietic stem cells do not transdifferentiate into cardiac myocytes in myocardial infarcts. *Nature*. 2004;428:664-668.
68. Balsam LB, Wagers AJ, Christensen JL, Kofidis T, Weissman IL, Robbins RC. Haematopoietic stem cells adopt mature haematopoietic fates in ischaemic myocardium. *Nature*. 2004;428:668-673.
69. Beltrami AP, Barlucchi L, Torella D, Baker M, Limana F, Chimenti S, Kasahara H, Rota M, Musso E, Urbanek K, Leri A, Kajstura J, Nadal-Ginard B, Anversa P. Adult cardiac stem cells are multipotent and support myocardial regeneration. *Cell*. 2003;114:763-776.
70. Ghostine S, Carrion C, Souza LC, Richard P, Bruneval P, Vilquin JT, Pouzet B, Schwartz K, Menasche P, Hagege AA. Long-term efficacy of myoblast transplantation on regional structure and function after myocardial infarction. *Circulation*. 2002;106:1131-1136.
71. Pagani FD, DerSimonian H, Zawadzka A, Wetzel K, Edge AS, Jacoby DB, Dinsmore JH, Wright S, Aretz TH, Eisen HJ, Aaronson KD. Autologous skeletal myoblasts transplanted to ischemia-damaged myocardium in humans. Histological analysis of cell survival and differentiation. *J Am Coll Cardiol*. 2003;41:879-888.
72. Pouly J, Hagege AA, Vilquin JT, Bissery A, Rouche A, Bruneval P, Duboc D, Desnos M, Fiszman M, Fromes Y, Menasche P. Does the functional efficacy of skeletal myoblast transplantation extend to nonischemic cardiomyopathy? *Circulation*. 2004;110:1626-1631.

73. Leri A, Kajstura J, Anversa P. Cardiac stem cells and mechanisms of myocardial regeneration. *Physiol Rev.* 2005;85:1373-1416.
74. Assmus B, Schachinger V, Teupe C, Britten M, Lehmann R, Dobert N, Grunwald F, Aicher A, Urbich C, Martin H, Hoelzer D, Dimmeler S, Zeiher AM. Transplantation of Progenitor Cells and Regeneration Enhancement in Acute Myocardial Infarction (TOPCARE-AMI). *Circulation.* 2002;106:3009-3017.
75. Schachinger V, Assmus B, Britten MB, Honold J, Lehmann R, Teupe C, Abolmaali ND, Vogl TJ, Hofmann WK, Martin H, Dimmeler S, Zeiher AM. Transplantation of progenitor cells and regeneration enhancement in acute myocardial infarction: final one-year results of the TOPCARE-AMI Trial. *J Am Coll Cardiol.* 2004;44:1690-1699.
76. Assmus B, Schachinger V, Teupe C, Britten M, Lehmann R, Dobert N, Grunwald F, Aicher A, Urbich C, Martin H, Hoelzer D, Dimmeler S, Zeiher AM. Transplantation of Progenitor Cells and Regeneration Enhancement in Acute Myocardial Infarction (TOPCARE-AMI). *Circulation.* 2002;106:3009-3017.
77. Schachinger V, Assmus B, Britten MB, Honold J, Lehmann R, Teupe C, Abolmaali ND, Vogl TJ, Hofmann WK, Martin H, Dimmeler S, Zeiher AM. Transplantation of progenitor cells and regeneration enhancement in acute myocardial infarction: final one-year results of the TOPCARE-AMI Trial. *J Am Coll Cardiol.* 2004;44:1690-1699.
78. Menasche P, Hagege AA, Vilquin JT, Desnos M, Abergel E, Pouzet B, Bel A, Sarateanu S, Scorsin M, Schwartz K, Bruneval P, Benbunan M, Marolleau JP, Duboc D. Autologous skeletal myoblast transplantation for severe postinfarction left ventricular dysfunction. *J Am Coll Cardiol.* 2003;41:1078-1083.
79. Kang HJ, Kim HS, Zhang SY, Park KW, Cho HJ, Koo BK, Kim YJ, Soo LD, Sohn DW, Han KS, Oh BH, Lee MM, Park YB. Effects of intracoronary infusion of peripheral

blood stem-cells mobilised with granulocyte-colony stimulating factor on left ventricular systolic function and restenosis after coronary stenting in myocardial infarction: the MAGIC cell randomised clinical trial. *Lancet*. 2004;363:751-756.

80. Meyer GP, Wollert KC, Lotz J, Steffens J, Lippolt P, Fichtner S, Hecker H, Schaefer A, Arseniev L, Hertenstein B, Ganser A, Drexler H. Intracoronary bone marrow cell transfer after myocardial infarction: eighteen months' follow-up data from the randomized, controlled BOOST (BOne marrOw transfer to enhance ST-elevation infarct regeneration) trial. *Circulation*. 2006;113:1287-1294.
81. Chachques JC, Acar C, Herreros J, Trainini JC, Prosper F, D'Attellis N, Fabiani JN, Carpentier AF. Cellular cardiomyoplasty: clinical application. *Ann Thorac Surg*. 2004;77:1121-1130.
82. Menasche P. Current status and future prospects for cell transplantation to prevent congestive heart failure. *Semin Thorac Cardiovasc Surg*. 2008;20:131-137.
83. Wollert KC. Cell therapy for acute myocardial infarction. *Curr Opin Pharmacol*. 2008;8:202-210.

JUSTIFICATIVAS

I - Dentre os fatores que podem interferir com o processo de hipertrofia ventricular pós-infarto e conseqüente disfunção cardíaca, as interações entre o processo inflamatório e de estresse oxidativo, progredindo para um quadro de IC, poderiam ser melhor exploradas em janelas temporais mais precoces após o insulto isquêmico.

II - O uso de células-tronco adjuvante a tratamentos já otimizados é, certamente, uma abordagem terapêutica a ser considerada, porém, sua melhor utilização depende de um maior conhecimento dos mecanismos de interação dos processos que permeiam seu desempenho no tecido miocárdico, seja por proliferação, fusão, transdiferenciação ou efeitos parácrinos.

HIPOTESES

I - A janela temporal de 48 horas pós-infarto permitiria avaliar o papel do estresse oxidativo na gênese do remodelamento ventricular, sendo o H_2O_2 um modulador dos processos que alteram a função cardíaca precocemente.

II - Neste contexto, o tratamento com células-tronco de medula óssea seria capaz de modular a função cardíaca, podendo retardar o início do remodelamento ventricular, através dos seus efeitos parácrinos sobre a hipertrofia ventricular e o processo inflamatório.

OBJETIVO GERAL

Avaliar o perfil do estresse oxidativo e sua associação com a função ventricular em 48 horas após o insulto isquêmico, num modelo experimental de IAM, analisando sua correlação com os efeitos parácrinos do tratamento com terapia celular com células da medula óssea.

Objetivos específicos

Artigo 01:

Avaliar precocemente (48 horas) pós-IAM o perfil de estresse oxidativo e sua associação com parâmetros ecocardiográficos de função ventricular em ratos Wistar.

Artigo 02:

Analisar os efeitos do uso de terapia celular utilizando células da medula óssea em modelo de IAM, 48 horas após a lesão, avaliando parâmetros ecocardiográficos de função ventricular, perfil oxidativo, inflamatório e apoptótico no miocárdio.

Artigo 1

Early oxidative stress profile and left ventricular function evaluation by echocardiography in rats at 48h post-experimental infarction

Avaliação Precoce do Perfil de Estresse Oxidativo e Função Ventricular por Ecocardiografia em Ratos 48 horas Pós-Infarto Experimental

Early oxidative stress profile and left ventricular function evaluation by echocardiography in rats at 48h post-experimental infarction

Cardiovascular Laboratory – Research Centre,
Hospital de Clínicas de Porto Alegre
Porto Alegre - RS, BRAZIL

Abstract

Background: Events occurring subsequent to acute myocardial infarction (AMI) are partially determinants of the cardiac damage extent later on. The role of redox balance in the post-ischemic cardiac tissue may be critical in this process.

Objectives: To assess cardiac function and its correlation with redox balance in cardiac tissue 48 hours post-experimental AMI.

Methods: Male Wistar rats, 8-week-old (n=6/group), weighing 229±24g, were randomized in two groups: Sham-operated (S) and AMI. AMI was produced in rats via ligation of the left coronary artery. Cardiac function parameters were evaluated by echocardiography 48h later. Oxidative profile was studied by measuring antioxidant enzyme activities of superoxide dismutase (SOD), catalase (CAT), glutathione peroxidase (GPx) and peroxiredoxine 6 (Prx-6). Oxidative damage was quantified by protein oxidation (carbonyls), lipid peroxidation (chemiluminescence - CL), reduced (GSH) and oxidized (GSSG) glutathione ratio and hydrogen peroxide (H₂O₂) concentration by spectrophotometer.

Results: Ejection fraction (EF) was lower in the infarct group: AMI (51±5%) vs. S (77±6%) (p=0.0001). Hydrogen peroxide values (H₂O₂) (nmol/mg protein) was diminished 48 hours post-AMI: AMI (0.022 ± 0.005) vs. S (0.032 ± 0.008) (p=0.024). We found a correlation between reduced/oxidized glutathione ratio (GSH/GSSG) and EF (r=0.79; p=0.009) at 48 hours post-MI. CL and carbonyls were not different between groups.

Conclusion: These data suggest that the loss of myocardial function and impaired redox balance may be associated with the activation of mechanisms that trigger the process of ventricular remodeling in heart failure. Moreover, we speculate that countervailing survival mechanisms act against H₂O₂ in order to maintain cardiac function in this early temporal window following AMI.

Key words: heart failure, redox balance, hydrogen peroxide.

Introduction

Subsequent to acute myocardial infarction (AMI), the heart undergoes a remodeling process that includes hypertrophy of surviving myocytes and hyperplasia of non-myocytes [1;2].

During left ventricular (LV) remodeling, the expression of several growth factors and cytokines is activated [3;4]. ROS (reactive oxygen species) are involved in modulating the activity of specific transcription factors, such as NF-κB [5;6], which are responsible for the

transcription of inflammatory cytokines. Besides modulating inflammatory processes, ROS have been shown to activate matrix metalloproteinases (MMPs) in cardiac fibroblasts [7]. In a model of MMP-2 knockout mice, a significant improvement in post-AMI survival was observed [8]. Thus, because MMPs can be activated by ROS, a proposed mechanism for LV remodeling is the activation of MMPs secondary to increased ROS production following injury [9].

An adequate oxygen supply is necessary to sustain cell viability and oxygen

metabolism is also central to the generation of ROS, which participate as benevolent molecules in many cellular functions, such as cell signaling process, but can also induce irreversible cellular damage [10].

Reactive oxygen species can oxidize membrane phospholipids, proteins, and DNA and are implicated in a wide range of pathological conditions. Toxic effects of ROS can be abrogated by enzymatic scavengers, as well as by non-enzymatic antioxidants [11]. For instance, H₂O₂ is neutralized by the enzymes glutathione peroxidase (GPx) and catalase (CAT).

Glutathione peroxidase, a selenium-containing enzyme that catalyzes removal of H₂O₂ through oxidation of reduced glutathione (GSH), and is recycled from oxidized glutathione (GSSG) by glutathione reductase (GRed) [12]. Similar to GPx, thioredoxin (Trx) complements the GSH system by protecting against ROS toxicity. GSH and Trx both function in the reduction of peroxides through the action of multiple GSH peroxidases and Trx peroxidases (peroxiredoxins), respectively [13].

The peroxiredoxin (Prx) superfamily, expressed in all the vital organs, including the heart [14], possesses H₂O₂ scavenging activities and also removes hydroperoxides [15]. Thus, the regulation of redox status is essential for maintaining cellular homeostasis, and can be compromised by injurious events such as cardiac ischemia. Increased oxidative stress results in a phenotype characterized by hypertrophy and apoptosis in isolated cardiac myocytes. Although these responses initially serve as an adaptative process, ultimately are often accompanied by depressed contractile function [16].

The importance of redox status in the development of heart failure subsequent to MI is evident from the association that both increased myocardial oxidative stress, as well as an antioxidant deficit are correlated with cardiac dysfunction at different stages of

failure [17]. Although many studies have explored the mechanisms of ventricular remodeling, relatively little is known regarding the role of redox balance in cardiac cells post-ischemia during the very early stages of heart failure.

In this study, we evaluated multiple parameters of cardiac function via echocardiography and its correlation with oxidative stress and antioxidant reserve in cardiac tissue examined 48 hours post-experimental MI.

Material and Methods

Animals and Groups

We studied male Wistar rats at the age of 8 weeks (n=6/group), weighing 229±24g. Animals were maintained in compliance with the "Principles of Laboratory Animal Care" formulated by the National Institutes of Health (publication No. 96-23, revised, 1996).

The study was approved by the ethics and research committee of Hospital de Clínicas de Porto Alegre. Animals were randomized in two groups: (a) sham-operated (**S**), with fictitious myocardial infarction surgery, and (b) acute myocardial infarction (**AMI**), with surgical procedure to induce myocardial infarction. All animals were maintained at temperatures ranging from 20°C to 25°C and in light/dark cycles of 12 hours and fed *ad libitum* with rat chow.

Myocardial Infarction Surgery

Myocardial infarction was induced according to a previously described procedure [18] and adapted in our laboratory. Briefly, animals were placed in dorsal decubitus position and anesthetized with xylazine (0.67mg/Kg i.p.) and ketamine (0.33 mg/Kg i.p.). Following orotracheal intubation, animals were submitted to mechanical ventilation (Harvard ventilator, Model 683). Thoracotomy

was performed without exteriorization of the heart. The left anterior descending coronary artery was occluded with a 6-0 mononylon. The thoracic cavity was closed with a 5-0 mononylon thread.

Echocardiogram

Animals underwent echocardiography prior to surgical interventions (baseline) and forty-eight hours following the surgical procedures. The EnVisor Philips system (Andover, MA, USA) was used, with a 12-13MHz transducer, at 2cm depth and fundamental and harmonic imaging.

Left ventricular dimensions – The end-diastolic and end-systolic transverse areas (cm²) were obtained by tracing the endocardial border at three levels: basal (at the tip of the mitral valve leaflets), middle (at the papillary muscle level) and apical (distal from the papillary muscle but before the final curve cavity) [19]. The end-diastolic and end-systolic diameters (cm) were also measured in the three planes using the M-Mode. The final value for each animal was taken as the mean of all three planes.

Myocardial infarction size – On each echocardiographic transverse plane, the arc corresponding to the infarcted segments (systolic movement akinesis and/or hypokinesis - AHR) and the total endocardial perimeter (EP) were measured at end-diastole. Infarction size (IS) was estimated [20] as % IS by using the following formula: IS= (AHR/EP) x 100.

Left Ventricular systolic function - Fractional area change (FAC) was calculated as follows: (FAC = diastolic area – systolic area / diastolic area). LV EF was calculated as: (End-diastolic volume – End-systolic volume / End-diastolic volume) x 100; end-diastolic end-systolic cavity volumes were calculated using Simpson's rule [21]. Ejected volume (EV) was determined by equation: $EV = (\pi R)^2 \times VTI$, where VTI is velocity time integral of the trace

of Doppler flow profile, R is radius cross section of aorta artery and π value is 3.1415. Cardiac output (CO) was obtained by the equation: CO = EV x Heart Rate (HR). LV fractional shortening (LVFS) was obtained by the equation: $LVFS = \frac{Dd - Sd}{Dd} \times 100$ (diastolic diameter – Dd; systolic diameter – Sd);

Left Ventricular diastolic function – Left ventricular diastolic function was assessed by E/A ratio, which was determined by dividing the peak velocity of the E wave by peak velocity of the A wave of the mitral diastolic flow profile.

Myocardial performance index (MPI) - MPI was obtained via the trace of Doppler flow profile as expressed by the following equation: $MPI = \frac{MFT - ET}{ET}$ (MF - mitral flow time; ET -ejection time of aortic artery) [22].

Left Ventricular Mass – Mass (in grams) was calculated according to the equation established by the American Society of Echocardiography $M(g) = 1.04[(Dd + AWDT + PWDT) - Dd^3]^3$ (anterior wall diastolic thickness – AWDT; posterior wall diastolic thickness – PWDT) [23;24].

Final values for all calculations for each animal were based on three transverse planes. Data were recorded in CD for later review and off-line analysis. Subsequent to echocardiography assessment, the animals were killed by cervical dislocation.

Tissue preparation

After animals were killed, hearts were rapidly excised, weighed, and homogenized (1.15% w/v KCl and phenyl methyl sulphonyl fluoride PMSF 20 mmol/L) in Ultra-Turrax. The resulting suspension was centrifuged at 600 g for 10 min at 0 - 4°C to remove nuclei and cell debris [25] and supernatant was used for oxidative stress measurements. Immediately following killing, left ventricle samples were removed and frozen at -80°C

for the evaluation of glutathione content and protein expression.

Determination of Lipid peroxidation

Tert-butyl-hydroperoxide-initiated chemiluminescence –

Chemiluminescence (CL) was measured in a liquid scintillation counter in the out-of-coincidence mode (LKB Rack Beta Liquid Scintillation Spectrometer 1215, LKB – Produkter AB, Sweden). Homogenates were placed in low-potassium vials at a protein concentration of 0.5-1.0 mg/mL in a reaction medium consisting of 120 mmol/L KCl and 30mmol/L phosphate buffer (pH=7.4). Measurements were started by the addition of 3 mmol/L tert-butyl hydroperoxide and data expressed as counts per second per milligram of protein (cps/mg protein) [26].

Carbonyl Assay

Tissue samples were incubated with 2,4 dinitrophenylhydrazine (DNPH 10 mol/L) in 2.5 mol/L HCl solution for 1 h at room temperature, in the dark. Samples were vortexed every 15 min. Subsequently, in tube samples, 20% TCA (w/v) solution was added, left in ice for 10 min and centrifuged for 5 min at 1000 g to collect protein precipitates. Another wash was performed with 10% TCA (w/v). The pellet was washed three times with ethanolethyl acetate (1:1) (v/v). The final precipitates were dissolved in 6 mol/L guanidine hydrochloride solution, incubated for 10 min at 37°C, and read at 360 nm [27].

Determination of antioxidant enzyme activities

Catalase (CAT) – CAT activity was determined by following the decrease in hydrogen peroxide (H₂O₂) absorbance at 240 nm. CAT activity was expressed as nanomoles of H₂O₂ reduced per minute per milligram of protein [28].

Superoxide dismutase (SOD) – SOD activity,

expressed as units per milligram of protein, was based on the inhibition of superoxide radical reaction with pyrogallol [29].

Glutathione peroxidase (GPx) – GPx activity expressed as nanomoles of peroxide/hydroperoxide reduced per minute per milligram of protein, was based on the consumption of NADPH a 480 nm [30].

Determination of oxidized and reduced glutathione concentration

To determine oxidized (GSSG) and reduced (GSH) glutathione concentration, tissue was deproteinized with 2 mol/L perchloric acid, centrifuged for 10 min at 1000 g and supernatant was neutralized with 2 mol/L potassium hydroxide. The reaction medium contained 100 mmol/L phosphate buffer (pH 7.2), 2 mmol/L NADPH, 0.2 U/mL glutathione reductase and 70 μmol/L 5,5' dithiobis (2-nitrobenzoic acid). To determine reduced glutathione, the supernatant was neutralized with 2 mol/L potassium hydroxide, reacted with 70 μmol/L 5,5' dithiobis (2-nitro benzoic acid), and read at 420 nm [31].

Determination of hydrogen peroxide (H₂O₂)

The assay was based on horseradish peroxidase (HRPO)-mediated oxidation of phenol red by H₂O₂. Ventricle slices were incubated for 30 min. at 37°C in 10 mmol/L phosphate buffer (NaCl 140 mmol/L and dextrose 5 mmol/L). Supernatants were transferred to tubes with 0.28 mmol/L phenol red and 8.5 U/mL HRPO. After a 5 min incubation, 1 mol/L NaOH was added and was read at 610 nm. The results were expressed in nanomoles H₂O₂ / g tissue [32].

Determination of nitric oxide (NO) metabolites (Nitrates)

Nitrates were determined as total nitrates (initial nitrite plus nitrite reduced from nitrate) after its reduction using nitrate reductase, from *Aspergillus* species in the

presence of NADPH. A standard curve was established with a set of serial dilutions (10^{-8} – 10^{-3} mol/L) of sodium nitrite. Results were expressed as mmol/mg protein [33].

Determination of protein concentration

Protein was measured by the method of Lowry [34], using bovine serum albumin as standard.

Western Blot Analysis

Tissue homogenization, electrophoresis, and protein transference were performed as described elsewhere [35;36]. Membranes were processed for immunodetection using rabbit anti-CAT polyclonal antibody, sheep anti-Cu/Zn SOD polyclonal antibody, and rabbit anti-Prx-6 as primary antibodies (Santa Cruz Biotechnology, Santa Cruz, CA).

The bound primary antibodies were detected using rabbit anti-sheep or goat anti-rabbit horseradish peroxidase-conjugate secondary antibodies and membranes were exposed for chemiluminescence. Autoradiographs were quantitatively analyzed with an image densitometer (Image Master DS Ci, Amersham Biosciences Europe, IT). Molecular weights of the bands were determined by referring to a standard molecular weight marker (RPN 800 rainbow full range Bio-Rad, CA, USA). Results from each membrane were normalized by the Ponceau red method [37].

Statistical analysis

Data are presented as mean \pm SD and were compared by Student's *t*-test. Simple linear regression analysis (Pearson correlation coefficient) was used to test associations between continuous variables. Tests with $P < 0.05$ were considered statistically significant. Data were analyzed using the Sigma Plot 11.0 program.

Results

Heart rate, infarction size and mortality

The mean HR after sedation during echocardiography was not significantly different between groups (243 ± 12 bpm for the S group and 222 ± 22 bpm for the AMI group). Area of infarction (% of circumference) was $46.91 \pm 8.55\%$ in the AMI group. Mortality occurring during or immediately after surgical procedure was around 10%.

Cardiac function

Systolic function - SD, EF, FAC, and LVFS were lower in rats with AMI than in the control animals ($p < 0.0001$) [Table 1] [Figure 1]. Both ET and EV were ($p = 0.0184$ and $p = 0.0498$, respectively) decreased in AMI group, although CO was not significantly different between groups [Table 1].

Diastolic function - Velocity of the E wave in the curve of diastolic mitral flow was not found to be different between groups, but the velocity of the A wave was lower in AMI group ($p = 0.0038$). E/A ratio was increased in the AMI group ($p = 0.0048$) [Figure 2]. In addition, a negative correlation between E/A ratio and GSH/GSSG ratio ($r = -0.71$; $p = 0.0321$) was found [Figure 4A]. The mitral diastolic flow deceleration time of E wave as well as mitral time flow was also not different between groups, [Table 1].

Myocardial performance index - MPI increased in the AMI group (0.24 ± 0.06 vs. 0.59 ± 0.14) ($p = 0.0009$) [Table 1]. A negative correlation was also found between MPI and EF ($r = -0.64$; $p = 0.036$).

Left Ventricular mass - The AMI group showed loss of LV mass compared to control ($p = 0.0146$) [Table 1].

Table 1 – Values of functional variables obtained by echocardiographic analysis

Variable	Groups		p Value
	S	AMI	
SD (cm)	0.27 ± 0.08	0.50 ± 0.03	0.0001
DD (cm)	0.64 ± 0.07	0.72 ± 0.05	0.0599
EF (%)	77 ± 7	51 ± 5	0.0001
FAC (cm)	0.71 ± 0.06	0.47 ± 0.06	0.0001
CO (mL/min)	87 ± 17	72 ± 28	0.3262
LVFS (%)	59 ± 10	30 ± 4	0.0001
E (m/sec)	1.24 ± 0.11	1.43 ± 0.24	0.1419
A (m/sec)	0.70 ± 0.13	0.45 ± 0.09	0.0038
E/A	1.78 ± 0.23	3.24 ± 0.84	0.0048
MDDT (msec)	46.2 ± 9.26	45.8 ± 6.59	0.9405
TF (msec)	125.2 ± 26.3	124.3 ± 15.7	0.9474
ET (msec)	108.6 ± 9.6	90.8 ± 10.7	0.0184
EV (mL)	0.366 ± 0.05	0.310 ± 0.1	0.0498
MPI	0.24 ± 0.06	0.59 ± 0.14	0.0009
LV Mass (g)	0.36 ± 0.06	0.28 ± 0.02	0.0146

Abbreviations: - S, Sham; SD, Systolic Diameter; DD, Diastolic Diameter; EF, Ejection Fraction; FAC, Fractional Area Change; CO, Cardiac Output; LVFS, Left Ventricular Fractional Shortening; E, E wave; A, A wave; E/A, E/A ratio; MDDT, Mitral Diastolic Flow Deceleration Time; TF, Time Flow; ET, Ejection Time; EV, Ejected Volume; MPI, Myocardial Performance Index. Data expressed as mean ± SD; p<0.05 vs. S group (Student's t-Test).

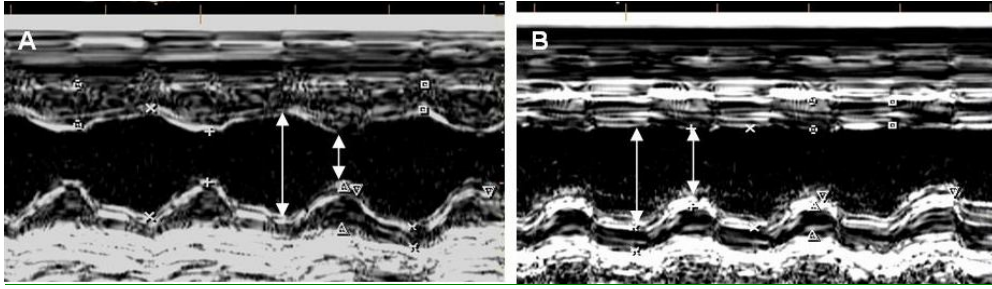


Figure 1 - Illustrative example of an M mode echocardiogram image of the left ventricle (LV) of the same animal before (A) and after (B) myocardial infarction (AMI group). Note the increase of the left ventricular cavity and loss of LV free wall contractility.

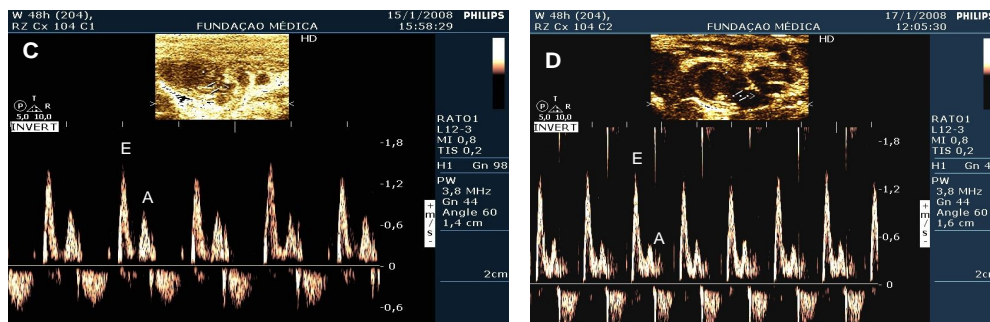


Figure 2 - Illustrative example of mitral inflow velocity profile determined by pulsed wave Doppler before (C) and after (D) acute myocardial infarction (AMI group). Note decreased A wave after acute myocardial infarction (D).

Oxidation products

Protein oxidation (carbonyls) and lipid peroxidation (CL) were not different in the AMI group compared to controls [Table 2].

Antioxidant enzyme activities and expression

Myocardial SOD and CAT activities were not different in the AMI group compared with controls. Similarly, the protein expression of SOD and CAT in the cardiac tissue was not different between the two groups [Table 2; Figure 3]. GPx activity was depressed by about 44% in the AMI group in relation to controls ($p=0.0025$). Conversely, Prx-6 protein expression was increased in the AMI group compared to control S ($p<0.0003$). A significant positive correlation between GPx and EF ($r = 0.71$; $p = 0.0162$) was also observed.

GSH/GSSG - reduced to oxidized glutathione ratio

GSH/GSSG was assessed as being significantly ($p=0.0226$) depressed by about 44% in the AMI group as compared to controls [Table 2]. A positive correlation existed between GSH/GSSG and EF ($r = 0.79$; $p = 0.0097$) [Figure 4C].

Hydrogen peroxide (H_2O_2)

Myocardial hydrogen peroxide concentration was lower ($p=0.0244$) in the AMI group as compared to controls [Table 2].

Nitric oxide (NO) metabolites (Nitrates)

NO metabolite levels in the myocardial tissue were not altered in the AMI group as compared to controls [Table 2].

Table 2 – Oxidative stress and antioxidant enzymes parameters

Variable	Groups		p Value
	S	AMI	
CL (cps/mg prot)	5526 ± 1228	6219 ± 969	0.3250
Carbonyl (nmol/mg prot)	2.23 ± 0.54	1.7 ± 0.41	0.0826
SOD activity (U/mg prot)	5.13 ± 2	5.22 ± 1.4	0.7561
CAT activity (µmol/mg prot)	40.57 ± 8.6	34.06 ± 9.01	0.2375
GPx (nmol/mg prot)	46.88 ± 9.0	26.32 ± 7.53	0.0025
GSH/GSSG ratio	14.61 ± 3.36	8.21 ± 3.81	0.0226
H ₂ O ₂ (nmol/mg prot)	0.032 ± 0.008	0.022 ± 0.005	0.0244
Nitrates (mmol/mg protein)	0.0448 ± 0.003	0.0429 ± 0.007	0.5738

Abbreviations – S, Sham; CL, chemiluminescence; superoxide dismutase (SOD), catalase (CAT), and glutathione peroxidase (GPx), reduced (GSH) and oxidized (GSSG) glutathione ratio, hydrogen peroxide (H₂O₂) and NO metabolites (Nitrates); Data expressed as mean ± SD; p<0.05 vs. S group (Student's t-Test).

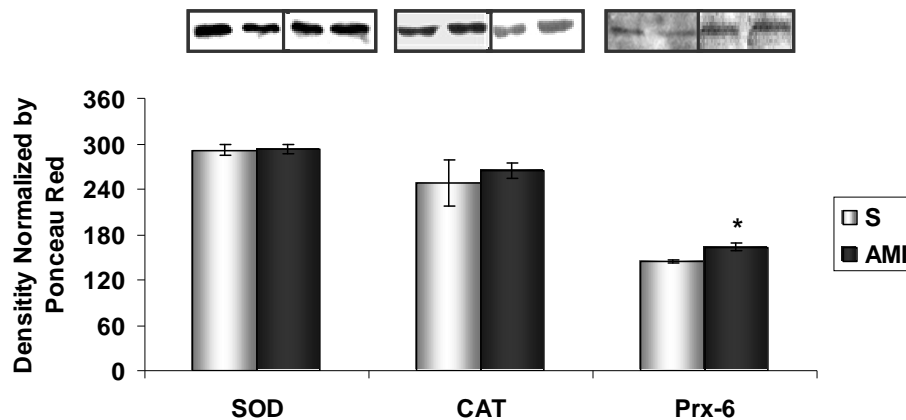


Figure 3 – Graph of Western blot analysis in cardiac homogenates using Cu/Zn SOD antibody, CAT antibody and Prx-6 antibody. p<0.05 as statistically significant. Note illustrative bands of blots on top part of graphs.

Abbreviations: S, Sham; AMI, acute myocardial infarction; SOD, superoxide dismutase; CAT, catalase; Prx-6, peroxiredoxin-6.

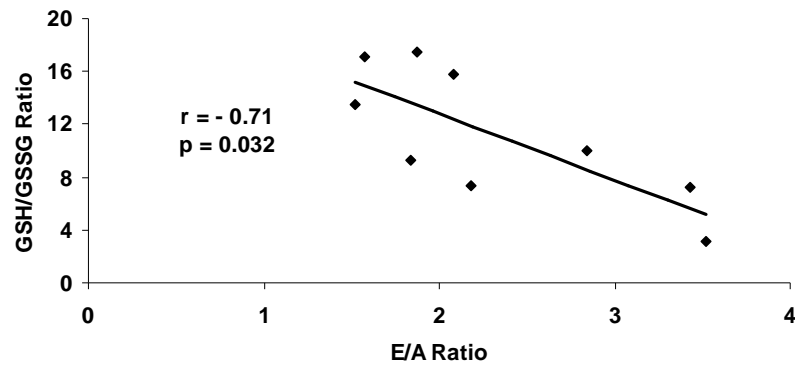


Figure 4 – A) Graph showing correlation between the E/A ratio and GSH/GSSG ratio.

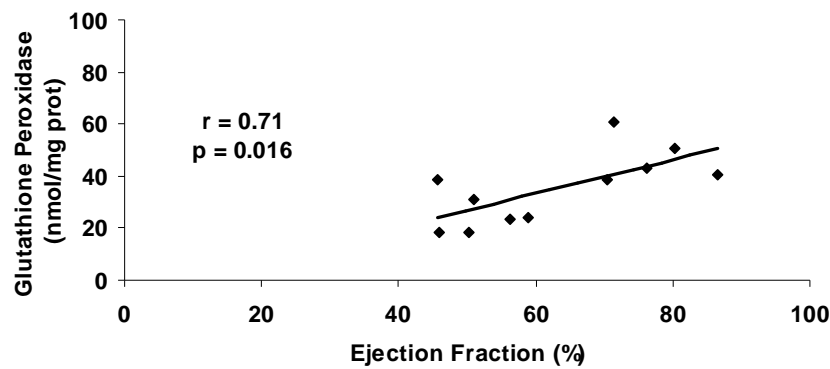


Figure 4 – B) Graph showing correlation between ejection fraction and glutathione peroxidase activity.

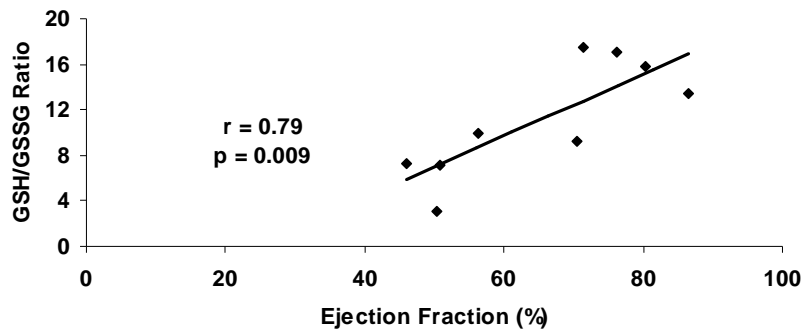


Figure 4 - C) Graph showing correlation between ejection fraction and GSH/GSSG ratio.

Discussion

In the present study, we found an early (48 hours post-MI) depression of cardiac function as reduced ejection fraction, fractional shortening and LV mass loss were

evident; however no significant alteration in cardiac output was observed. Also, from the analyses of redox status at this time point, we found that the steady-state myocardial H_2O_2 concentration was diminished, the activity of the antioxidant GPx was lower, and the

oxidative stress index, GSH/GSSG ratio, was decreased.

This apparent balance of various redox state contributors present in a decompensated cardiac scenario was also evident in functional readouts, where cardiac flow assessment, E/A ratio and ET were depressed in the AMI group, while TF and MDDT did not change. Moreover, MPI was found to be markedly increased and was significantly negatively correlated with EF. The clear reduction of LVFS characterizes an impairment of ventricular contractility associated with an expressive LV chamber enlargement, as can be seen by the enhanced systolic diameter.

Although diastolic diameter was not changed, an evident loss of systolic function was witnessed. Additionally, it was observed that although the LV rapid filling was normal, the slow filling was depressed and the EV was minor, showing that diastolic function was also depressed in the AMI group at this time point. A strong correlation between diastolic dysfunction (higher E/A ratio) and oxidative stress was also demonstrated (Figure 4A).

It has previously been shown that ROS generated in the immediate post-AMI period can also function to modulate cardiac inotropism, inducing cardiac hypertrophy and apoptosis. These events reduce calcium myofilament sensitivity and cardiac contractility, contributing to the development of heart failure [6].

While we did not find increased myocardial oxidative damage, as observed by protein oxidation and lipid peroxidation data, we did observe diminished antioxidant defenses through decreased GPx activity at 48 hours post-MI. GPx is an important enzyme that catalyzes the reduction of H₂O₂ and hydroperoxides, preventing the formation of other more toxic radicals, such as ·OH [38].

Furthermore, we found a positive correlation between GPx and EF, suggesting

a strong association between cardiac function and the activity of this enzyme. These data corroborate previous findings which demonstrated that GPx overexpression inhibits the development of LV remodeling and failure after AMI, which could contribute to the improved survival [38], attenuation of diastolic dysfunction, myocyte hypertrophy, and interstitial fibrosis in diabetes [39].

We also analyzed myocardial CAT activity and protein expression, but found no significant differences between groups. Studies suggest that CAT activity and expression have minor relevance to GPx in cardiac tissue [11]. We also did not note important differences in myocardial SOD activity or protein expression between groups, leading us to believe that O₂⁻ concentration is not significantly altered in our model.

Tissue production of O₂⁻ and, consequently, low levels of H₂O₂, are maintained by the basal activity of endothelial NADPH oxidases and by mitochondrial electron chain leakage, and is necessary for endothelial growth and proliferation [40]. Under pathological conditions such as AMI, agonist-induced activation of NADPH oxidase and the subsequent activation of xanthine oxidase, as well as the uncoupling of eNOS, result in the production of large quantities of H₂O₂, leading to cardiac dysfunction. For instance, when H₂O₂ diffuses to adjacent muscle tissue, it can induce hypertrophy [41].

Interestingly, myocardial concentration of H₂O₂ was diminished at 48 hours post-AMI in our study. We believe that this finding suggests countervailing survival mechanisms acting against H₂O₂ in order to maintain cardiac function in this temporal window following MI. Among these mechanisms are novel antioxidant proteins designated as peroxiredoxins (Prxs). Among six known mammalian Prxs, Prx-1, -2, -3, and -4 require the small redox protein thioredoxin (Trx) as an electron donor to remove H₂O₂. Prx-3 is

especially efficient as an antioxidant, perhaps because it can utilize lipid peroxides as well as H_2O_2 as substrates. This may also help to explain the minimization of lipid damage evident in our present CL data.

Moreover, Prx-3 overexpression was also associated with heart protection, reducing LV remodeling and heart failure progression in mice following AMI [42]. Importantly, Prx-3 functions not only to remove H_2O_2 formed after SOD-catalyzed dismutation reactions, but also detoxifies peroxynitrite [43].

This may also help to explain why we did not observe differences in nitrate level between groups. A key role of Prx-6 in ischemic injury has also been suggested. In a study of Prx-6^{-/-} mice subjected to 30 min of global ischemia followed by 120 min of reperfusion at normothermia, Prx6^{-/-} mice exhibited reduced post-ischemic ventricular recovery, increased infarct size, and increased cardiomyocyte apoptosis as compared with wild-type controls [44].

In our findings, we observed that Prx-6 was significantly increased in the AMI group compared with the control group, demonstrating that in an ischemic environment, during this time point, Prx-6 can also act as a reperfusion-independent H_2O_2 scavenger.

In the present study, we also observed a marked decrease in the GSH/GSSG ratio, possibly due to a depletion of GSH in cardiac tissue. Moreover, this redox imbalance was positively correlated with EF. In addition, the observed decrease in GPx activity may also result from decreased GSH concentration at later time points [45].

In summary, our data suggest that this period (48 hours post-AMI) represents a point at which compensated cardiac function begins to shift toward the progression to heart failure. Our results show a strong correlation between oxidative stress and cardiac function and that

H_2O_2 may play an important role in this potential transitional phase.

Conclusions

It is widely accepted that events transpiring in the period immediately following cardiac injuries, such as those imparted by AMI, have important implications for ultimate functional capacity and potential for progression to heart failure.

Our evaluation of cardiac function and redox status at the relatively early period of 48 hours post-MI suggest that it may represent a point of critical transition from a compensated to decompensated state. In particular, our data show a depressed GPx and GSH/GSSG ratio, indicating redox imbalance, which may pave the way for activation of inflammatory and apoptotic responses, which represent key next steps in the process of ventricular remodeling.

Our observations of differential H_2O_2 concentration lead us to believe that the above-mentioned transition may be dependent on, or otherwise influenced by H_2O_2 levels. In this study, the low H_2O_2 concentrations noted may act as a 'sensor' for survival pathway activation within this timeframe following AMI. This 'sensor' could be regulated by Prx-6 in this time point.

To conclude, this temporal window seems to be an important period in which we may better exploit the role and contribution of oxidative stress as a trigger for signaling in the processes leading to heart failure.

Acknowledgements

We would like to thank Ms. Tania R. G. Fernandes for technical assistance and to Andreia C. Taffarel (Veterinary Medicine), Gabriela Nicolaidis (Medicine) and Rafael Dall'Alba (Biology), undergraduate students of UFRGS, for their generous contribution. This work was supported by HCPA-FIPE and CNPq grants.

References

- [1] Anversa P, Beghi C, Kikkawa Y, et al. Myocardial response to infarction in the rat. Morphometric measurement of infarct size and myocyte cellular hypertrophy. *Am J Pathol* 1985;118:484-92.
- [2] Weber KT, Brilla CG. Pathological hypertrophy and cardiac interstitium. Fibrosis and renin-angiotensin-aldosterone system. *Circulation* 1991;83:1849-65.
- [3] Hanatani A, Yoshiyama M, Kim S, et al. Inhibition by angiotensin II type 1 receptor antagonist of cardiac phenotypic modulation after myocardial infarction. *J Mol Cell Cardiol* 1995;27:1905-14.
- [4] Herskowitz A, Choi S, Ansari AA, et al. Cytokine mRNA expression in postischemic/reperfused myocardium. *Am J Pathol* 1995;146:419-28.
- [5] Storz P, Doppler H, Toker A. Protein kinase Cdelta selectively regulates protein kinase D-dependent activation of NF-kappaB in oxidative stress signaling. *Mol Cell Biol* 2004;24:2614-2626.
- [6] Giordano FJ. Oxygen, oxidative stress, hypoxia, and heart failure. *J Clin Invest*. 2005;115:500-08.
- [7] Siwik DA, Pagano PJ, Colucci WS. Oxidative stress regulates collagen synthesis and matrix metalloproteinase activity in cardiac fibroblasts. *Am J Physiol Cell Physiol* 2001;280:C53-C60.
- [8] Hayashidani S, Tsutsui H, Ikeuchi M, et al. Targeted deletion of MMP-2 attenuates early LV rupture and late remodeling after experimental myocardial infarction. *Am J Physiol Heart Circ Physiol* 2003;285:H1229-H1235.
- [9] Rajagopalan S, Meng XP, Ramasamy S, et al. Reactive oxygen species produced by macrophage-derived foam cells regulate the activity of vascular matrix metalloproteinases in vitro. Implications for atherosclerotic plaque stability. *J Clin Invest* 1996;98:2572-79.
- [10] Davies KJ. Oxidative stress: the paradox of aerobic life. *Biochem Soc Symp* 1995;61:1-31.
- [11] Tsutsui H. Mitochondrial oxidative stress and heart failure. *Intern Med* 2006;45:809-13.
- [12] Sawyer DB, Siwik DA, Xiao L, et al. Role of oxidative stress in myocardial hypertrophy and failure. *J Mol Cell Cardiol* 2002;34:379-88.
- [13] Watson WH, Yang X, Choi YE, Jones DP, Kehrer JP. Thioredoxin and its role in toxicology. *Toxicol Sci* 2004;78:3-14.
- [14] Fisher AB, Dodia C, Feinstein SI, et al. Altered lung phospholipid metabolism in mice with targeted deletion of lysosomal-type phospholipase A2. *J Lipid Res* 2005;46:1248-56.
- [15] Trachootham D, Lu W, Ogasawara MA, et al. Redox regulation of cell survival. *Antioxid Redox Signal* 2008;10:1343-74.
- [16] Siwik DA, Tzortzis JD, Pimental DR, et al. Inhibition of copper-zinc superoxide dismutase induces cell growth, hypertrophic phenotype, and apoptosis in neonatal rat cardiac myocytes in vitro. *Circ Res* 1999;85:147-53.
- [17] Hill MF, Singal PK. Antioxidant and oxidative stress changes during heart failure

- subsequent to myocardial infarction in rats. *Am J Pathol* 1996;148:291-00.
- [18]** Pfeffer MA, Pfeffer JM, Fishbein MC, et al. Myocardial infarct size and ventricular function in rats. *Circ Res* 1979;44:503-12.
- [19]** Nozawa E, Kanashiro RM, Murad N, et al. Performance of two-dimensional Doppler echocardiography for the assessment of infarct size and left ventricular function in rats. *Braz J Med Biol Res* 2006;39:687-95.
- [20]** Peron AP, Saraiva RM, Antonio EL, et al. Mechanical function is normal in remanent myocardium during the healing period of myocardial infarction--despite congestive heart failure. *Arq Bras Cardiol* 2006;86:105-12.
- [21]** Mercier JC, DiSessa TG, Jarmakani JM, et al. Two-dimensional echocardiographic assessment of left ventricular volumes and ejection fraction in children. *Circulation* 1982;65:962-69.
- [22]** Cury AF, Bonilha A, Saraiva R, et al. Myocardial performance index in female rats with myocardial infarction: relationship with ventricular function parameters by Doppler echocardiography. *J Am Soc Echocardiogr* 2005;18:454-60.
- [23]** Litwin SE, Katz SE, Morgan JP, et al. Serial echocardiographic assessment of left ventricular geometry and function after large myocardial infarction in the rat. *Circulation* 1994;89:345-54.
- [24]** Moises VA, Ferreira RL, Nozawa E, et al. Structural and functional characteristics of rat hearts with and without myocardial infarct. Initial experience with Doppler echocardiography. *Arq Bras Cardiol* 2000;75:125-36.
- [25]** Llesuy SF, Milei J, Molina H, et al. Comparison of lipid peroxidation and myocardial damage induced by adriamycin and 4'-epiadriamycin in mice. *Tumori* 1985;71:241-49.
- [26]** Gonzalez FB, Llesuy S, Boveris A. Hydroperoxide-initiated chemiluminescence: an assay for oxidative stress in biopsies of heart, liver, and muscle. *Free Radic Biol Med* 1991;10:93-00.
- [27]** Reznick AZ, Packer L. Oxidative damage to proteins: spectrophotometric method for carbonyl assay. *Methods Enzymol* 1994;233:357-63.
- [28]** Aebi H. Catalase in vitro. *Methods Enzymol* 1984;105:121-26.
- [29]** Marklund, S. Handbook of Methods for Oxygen Radical Research CRC. Pyrogallol autooxidation. 243-247. 1985. Press Boca Raton.
- [30]** Flohe L, Gunzler WA. Assays of glutathione peroxidase. *Methods Enzymol* 1984;105:114-21.
- [31]** Akerboom TP, Sies H. Assay of glutathione, glutathione disulfide, and glutathione mixed disulfides in biological samples. *Methods Enzymol* 1981;77:373-82.
- [32]** Pick E, Keisari Y. A simple colorimetric method for the measurement of hydrogen peroxide produced by cells in culture. *J Immunol Methods* 1980;38:161-70.
- [33]** Granger DL, Anstey NM, Miller WC, et al. Measuring nitric oxide production in human clinical studies. *Methods Enzymol* 1999;301:49-61.

- [34] Lowry OH, Rosebrogh NJ, Farr AL, et al. Protein measurement with the Folin phenol reagent. *J Biol Chem* 1951;193:265-75.
- [35] Araujo AS, Ribeiro MF, Enzweiler A, et al. Myocardial antioxidant enzyme activities and concentration and glutathione metabolism in experimental hyperthyroidism. *Mol Cell Endocrinol* 2006;249:133-39.
- [36] Laemmli UK. Cleavage of structural proteins during the assembly of the head of bacteriophage T4. *Nature* 1970;227:680-85.
- [37] Klein D, Kern RM, Sokol RZ. A method for quantification and correction of proteins after transfer to immobilization membranes. *Biochem Mol Biol Int* 1995;36:59-66.
- [38] Shiomi T, Tsutsui H, Matsusaka H, et al. Overexpression of glutathione peroxidase prevents left ventricular remodeling and failure after myocardial infarction in mice. *Circulation* 2004;109:544-49.
- [39] Matsushima S, Kinugawa S, Ide T, et al. Overexpression of glutathione peroxidase attenuates myocardial remodeling and preserves diastolic function in diabetic heart. *Am J Physiol Heart Circ Physiol* 2006;291:H2237-H2245.
- [40] Cai H, Griendling KK, Harrison DG. The vascular NAD(P)H oxidases as therapeutic targets in cardiovascular diseases. *Trends Pharmacol Sci* 2003;24:471-78.
- [41] Cai H. Hydrogen peroxide regulation of endothelial function: origins, mechanisms, and consequences. *Cardiovasc Res* 2005;68:26-36.
- [42] Matsushima S, Ide T, Yamato M, et al. Overexpression of mitochondrial peroxiredoxin-3 prevents left ventricular remodeling and failure after myocardial infarction in mice. *Circulation* 2006;113:1779-86.
- [43] Bryk R, Griffin P, Nathan C. Peroxynitrite reductase activity of bacterial peroxiredoxins. *Nature*. 2000;407:211-15.
- [44] Nagy N, Malik G, Fisher AB, et al. Targeted disruption of peroxiredoxin 6 gene renders the heart vulnerable to ischemia-reperfusion injury. *Am J Physiol Heart Circ Physiol* 2006;291:H2636-H2640.
- [45] Khaper N, Singal PK. Modulation of oxidative stress by a selective inhibition of angiotensin II type 1 receptors in MI rats. *J Am Coll Cardiol* 2001;37:1461-66.

Artigo 2

Paracrine Effects of Early Bone Marrow Cells Treatment in Experimental Myocardial Infarction in Rats: Tissue Evaluation of Inflammatory Process, Redox Status and Echocardiographic Parameters

Efeitos Parácrinos do Tratamento Precoce com Células-Tronco de Medula Óssea no Infarto do Miocárdio Experimental em Ratos: Avaliação Tecidual do Processo Inflamatório, Estado Redox e Parâmetros Ecocardiográficos

Paracrine Effects of Early Bone Marrow Cells Treatment in Experimental Myocardial Infarction in Rats: Tissue Evaluation of Inflammatory Process, Redox Status and Echocardiographic Parameters

Cardiovascular Laboratory – Research Centre,
Hospital de Clínicas de Porto Alegre
Porto Alegre - RS, BRAZIL

Abstract

Background: Association among redox unbalance, inflammation and apoptosis are associated with cardiac dysfunction post-acute myocardial infarction (AMI). Transplant of bone marrow cells (BMC) can exert beneficial effects through paracrine actions on the host tissue.

Objective: To assess cardiac function and its correlation with redox balance, inflammatory process and apoptosis in cardiac tissue 48 hours post-experimental AMI treated with cellular therapy.

Methods: Male 8-week-old Wistar rats were randomized into four groups: Sham-operated (S) with fictitious myocardial infarction surgery; AMI; S + treatment (ST) and AMI + treatment (AMIT). Induction of AMI was accomplished through ligation of the left anterior descending coronary artery (LAD), with open-chest under mechanic ventilation. Determination of ejection fraction (EF) and akinetic or hypokinetic regions (AHR) were evaluated by echocardiography. Tumor necrosis factor (TNF)- α , Interleukin(IL)-6 and Caspase-3 were measured by Western Blot, and the reduced and oxidized glutathione ratio (GSH/GSSG) were measured by spectrophotometer.

Results: Infarcted area (%) was not different between groups AMI (52.8 \pm 5.7) vs. AMIT (54.2 \pm 4.3). EF (%) was lower in the infarcted groups: AMI (51 \pm 5%) vs. S (74 \pm 7%) (p=0.001) and AMIT (56 \pm 10%) vs. ST groups (73 \pm 3%) (p=0.001). Oxidative stress assessed by GSH/GSSG ratio was increased in infarcted groups, AMI (8.21 \pm 3.8) vs. S (14.61 \pm 3.4) (p<0.05), AMIT (2.1 \pm 0.7) vs. ST (4.7 \pm 1.5) (p<0.05) and with treatment the oxidative stress was high, AMIT (2.1 \pm 0.7) vs. AMI (8.21 \pm 3.8) (p<0.005), as well as caspase-3 expression. However, it was observed that BMC treatment was able to minimize ventricular hypertrophy (mg/g) in AMIT (2.86 \pm 0.2) vs. AMI group (3.40 \pm 0.6) (p<0.001) and minimize TNF- α and IL-6 expression in infarcted treated group. We found a positive correlation between ventricular hypertrophy and cytokines' expression of TNF- α (r=0.732; p=0.001), and IL-6 (r=0.720; p=0.001).

Conclusions: Our data suggest that BMC treatment was able of attenuate ventricular hypertrophy and reduced the expression of pro-inflammatory cytokines through its paracrine effects, at least in this time point.

Key words: oxidative stress, inflammation, cardiac hypertrophy, stem cell therapy, experimental infarction

Introduction

Considerable progress has been achieved in the search for new therapies for the management of acute myocardial infarction (AMI) and consequent heart failure (HF) due to

ventricular remodeling; nonetheless, HF continues to be a major world-wide problem¹.

Cell therapy has been proposed a stimulating approach to promote cardiac repair post-AMI, although clinical data have brought

somewhat disappoint long term results². Clearly in depth experimental studies are required to better understand multiple and distinct mechanisms involved in both ventricular remodeling and how cellular therapy may function in this scenario. In fact, several mechanisms have been proposed to explain the effects of cell therapy. These include cell transdifferentiation, cell fusion and/or paracrine effects.

Recent evidence suggests that transplanted cells can exert a beneficial influence through paracrine effects, secreting cytokines and growth factors that stimulate proliferation and differentiation of host tissue³.

Several studies have shown that the mechanical wall stress associated with myocardial infarction leads to the prompt production in the myocardium of pro-inflammatory cytokines such as tumor necrosis factor (TNF)- α and Interleukin (IL)-6. These cytokines are rapidly released in the central ischemic zone during infarction but are usually maximal in the ischemic zone border^{4,5}. Similarly, it has been proposed an association between increased myocardial oxidative stress and an antioxidant deficit correlating with cardiac dysfunction at different stages of failure⁶.

Excessive reactive oxygen species (ROS) may derive from intracellular sources such as mitochondrial dysfunction or may be secreted by infiltrating cells during the inflammatory response to the ischemic insult, as reviewed by Ungvári and colleagues⁷.

Isolated adult rat cardiomyocytes exposed to different TNF- α concentrations showed that this exposure caused a significant decrease in both protein and mRNA for manganese (Mn) superoxide dismutase (SOD) and catalase (CAT), as well as, glutathione peroxidase protein (GPx), increased intracellular ROS and lipid peroxidation⁸.

Recently, oxidative stress was shown to trigger cardiomyocyte apoptosis in myocardial infarction ischemia/reperfusion injury, atherosclerosis, and heart failure⁹⁻¹¹.

Bone marrow cells (BMC) administered after coronary ligation in mice showed that, four days after myocardial infarction, BMC were found within injured myocardium. However, cardiomyocytes were observed in low number within per-infarct area in BMC group, which suggests that other mechanisms than differentiation and fusion may be responsible for the beneficial effects of cell therapy¹².

Ventricular remodeling is characterized by changes in left ventricular (LV) geometry, mass, volume, and function, which include hypertrophy and cellular apoptosis of cardiomyocytes, in response to myocardial injury or alteration in load¹³.

Although the role of oxidative stress and inflammatory process are considered part of the cardiac injury process leading to remodeling, the effects of early treatment with BMC in the redox status and its consequences on inflammatory pathways and cell cycle remain unclear.

In this study, we aimed to evaluate the profile of oxidative stress, inflammatory process and apoptosis in myocardial tissue, submitted to BMC treatment, 48 hours post- infarction.

Material and Methods

Animals and Groups

We studied male Wistar rats 8-week-old. Animals were kept at Experimental Animal Unit of Research Centre of Hospital de Clínicas de Porto Alegre. All animals were treated in accordance with the *Guidelines for the Care and Use of Laboratory Animals* prepared by the National Academy of Sciences and published by the National Institutes of Health (NIH publication no. 85-23, Revised 1996). The study was

approved by the Research ethics committee of Hospital de Clínicas de Porto Alegre. Animals were randomized in four groups: Sham-operated (**S**) with fictitious myocardial infarction surgery; Acute Myocardial Infarction (**AMI**); S + treatment (**ST**) and MI + treatment (**AMIT**). All animals were kept in cages in room with temperature ranging from 20°C to 25°C and light/dark cycles of 12 hours, and fed *ad libitum* with rat chow.

Myocardial Infarction Surgery

Myocardial infarction was induced according to a procedure previously described in the literature and adapted in our laboratory¹⁴. Briefly, animals were placed in dorsal decubitus position and anesthetized with xilazine (0.67mg/Kg) and ketamine (0.33 mg/Kg) administered intraperitoneally.

Then, following orotracheal intubation, animals were submitted to mechanical ventilation with Harvard ventilator, Model 683 (frequency: 60m/min, tidal volume: 1.5 mL). Next, a surgical incision was performed in the skin along the left sternal margin, and division of pectoralis and transverses muscle was performed. Thoracotomy was performed at the 2nd intercostal space and thorax was opened, without exteriorization of the heart. The left anterior descending coronary artery (LAD) was identified and occluded with a 6-0 mononylon suture between the left atrial appendage margin and the pulmonary artery. Next, the thoracic cavity was closed with a 5-0 mononylon thread, muscles were repositioned and skin sutured. All animals received analgesic after surgical procedure (dipirone 0.1mL-*i.m.*).

Isolation and staining of BMC

Bone marrow cells from male donors were obtained as follows: after killing animals in CO₂ chamber, the tibia and femur were flushed with cell culture media (DMEM, Invitrogen, USA)

and mononuclear bone marrow cell fraction was isolated by centrifugation using FICOLL (GE-Healthcare, USA) gradient¹⁵. The cells were then stained with DAPI (4-6-diamine-2-phenylindole dihydrochloride, Roche Mannheim, Germany)¹⁶, 2.7 mg/mL. Cells were counted using Neubauer chamber and Trypan Blue exclusion test to verify cell viability, and adjusted to 2x10⁶ cells/mL final concentration.

Cell Transplantation

Five injections of 10µl (cells concentration) were administered after LAD occlusion or fictitious myocardial infarction surgery in five different sites around ischemic size of LV free wall (ST and AMIT groups).

Flow Cytometry Analysis

Approximately 2 x 10⁶ mononuclear BMC were prepared. They were placed in sterile tubes and washed twice by centrifugation at 2000 rpm for 5 minutes at 4°C. BMC were then resuspended in 200 µL of PBS and incubated for 20 minutes at 4°C with FITC-anti-CD45 (CALTAG lab. CA,USA) and PE-anti-CD34 (Santa Cruz Biotechnology, Santa Cruz, CA) for characterization of hematopoietic stem cells through the ISHAGE protocol¹⁷. Anti-KDR (Abcam, Inc, CA, USA) and PE-anti-CD34 (Santa Cruz Biotechnology, Santa Cruz, CA) were used to quantify endothelial precursors cells¹⁸. We also characterized the mesenchymal stem cell population in our sample performing triple staining for FITC-anti-CD44 (Abcam Inc, CA, USA), PE-anti-CD71 (AbD Serotec - Munich, DEU) and PECy5-anti- CD29 (BioLegend, San Diego, CA)¹⁹.

All assays were conducted using antibodies' concentrations as recommended by manufactures. Phycoerythrin-PE and FITC mouse anti-rat IgG1, IgG2a and IgM were used as isotype controls. After antibody incubation,

lysis solution (1 mL) was added for 15 minutes to hemolyze erythrocytes; then 1 mL of PBS was added for another 15 minutes to stop the hemolytic treatment. Cells were collected and washed with PBS by centrifugation and 500 μ L of PBS was added to the cell suspension. Analysis was carried out with the BD FACS-Calibur flow cytometry system with a one-laser system that is capable to detect three fluorochromes excited by the 488 nm laser in a multiparameter manner. The samples were read in the cell quest and PAINT-A-GATE software.

Echocardiogram

Before surgical interventions (baseline evaluation) and forty-eight hours after surgical procedures, animals underwent echocardiography. Animals were placed in left lateral decubitus position (45°) to obtain cardiac images. EnVisor HD System, Philips Medical (Andover, MA, USA) was used, with a 12-13MHz transducer, at 2cm depth and fundamental and harmonic imaging. Images were captured by a trained operator with experience in gruel animal echocardiography.

Left ventricular dimensions – The end-diastolic and end-systolic transverse areas (cm²) were obtained by tracing the endocardial border at three levels: basal (at the tip of the mitral valve leaflets), middle (at the papillary muscle level) and apical (distal from the papillary muscle but before final curve cavity)²⁰. End-diastolic and end-systolic diameters (cm) were measured using the M-Mode, also in the three planes. Final value for each animal was obtained by the average of these all three planes.

Myocardial infarction size – On each echocardiographic transverse plane (basal, middle and apical) the arc corresponding to the segments with infarction (regions or segments of the myocardium showing one the following changes in myocardial kinetics: systolic

movement akinesis and/or hypokinesis - AHR) and to the total endocardial perimeter (EP) were measured at end-diastole. Infarction size (IS) was estimated as %IS = (AHR/EP) x 100²¹.

LV systolic function - LV ejection fraction (EF) was calculated as: (End-diastolic volume – End-systolic volume / End-diastolic volume) x 100; end-diastolic and end-systolic cavity volumes were calculated using Simpson's rule²². Left ventricular fractional shortening (LVFS) was obtained by equation: LVFS = Dd – Sd/Dd x 100 (diastolic diameter – Dd; systolic diameter – Sd);

LV Mass – Mass (in grams) was calculated according to the equation established by the American Society of Echocardiography $M(g)=1.04 [(Dd + AWDT + PWDT) - Dd]^3$ (anterior wall diastolic thickness – AWDT; posterior wall diastolic thickness – PWDT)^{23;24}.

Final value volumes to all calculations for each animal were based on three transverse planes. Two-dimensional images and tracings of the M-Mode were recorded in CD for later review and off-line analysis.

Organs weight data

After undergoing echocardiography, animals were killed by anesthesia with xylazine (0.67 mg/Kg) and ketamine (0.33 mg/Kg), followed by cervical dislocation and underwent thoracotomy for heart and lung removal, as well as open peritoneum was opened for liver removal. In order to obtain the wet/dry weight ratio of the lungs and liver, these organs were removed and freed from adhering tissue. In each case, the tissue was weighed and placed in the oven (100°C) for 72 h. The hearts were weighted (only ventricles) to analyze ventricular hypertrophy. Hypertrophy was calculated by left and right ventricles/body weight.

Hemodynamic and tissue weight determinations

After undergoing echocardiography, the animals were placed to allow pressure measurements (MP100 - Biopac Systems, Inc – CO) through a catheter inserted into the right carotid artery and then advanced into the left ventricle. Left ventricular end-diastolic (LVEDP) and left ventricular peak systolic pressures (LVSP) were recorded for an offline analysis. After these assessments, the rats were killed and the heart and other organs removed for further studies.

Cardiac tissue preparation for analysis of oxidative processes

After completing cardiac hemodynamic measurements, rats were killed and hearts were rapidly excised, weighted, and immediately frozen in liquid nitrogen and stored at -80°C for the evaluation of glutathione content and protein expression or homogenized in 1.15% w/v KCl and phenyl methyl sulphonyl fluoride PMSF 20 mmol/L in Ultra-Turrax.

The resulting suspension was centrifuged at 600 g for 10 min at $0 - 4^{\circ}\text{C}$ to remove the nuclei and cell debris²⁵ and supernatants were used for oxidative stress measurements. Immediately following killing, and prior to homogenization, cardiac tissue samples were removed and frozen at -80°C for the evaluation of glutathione content and protein expression.

*Determination of lipid peroxidation**Tert-butyl-hydroperoxide-initiated chemiluminescence*

Chemiluminescence (CL) was measured in a liquid scintillation counter in the out-of-coincidence mode (LKB Rack Beta Liquid Scintillation Spectrometer 1215, LKB – Produkter AB, Sweden). Homogenates were placed in low-potassium vials at a protein concentration of 0.5-1.0 mg/mL in a reaction medium consisting of

120 mmol/L KCl, 30 mmol/L phosphate buffer (pH=7.4). Measurements were started by the addition of 3 mmol/L tert-butyl hydroperoxide and data expressed as counts per second per milligram of protein (cps/mg protein)²⁶.

Determination of antioxidant enzyme activities

Catalase (CAT) – activity was determined by following the decrease in hydrogen peroxide (H_2O_2) absorbance at 240nm. It was expressed as nanomol of H_2O_2 reduced per minute per milligram of protein²⁷.

Superoxide dismutase (SOD) activity, expressed as units per milligram of protein, was based on the inhibition of superoxide radical reaction with pyrogallol²⁸.

Glutathione peroxidase (GPx) – activity expressed as nanomols of peroxide/hydroperoxide reduced per minute per milligram of protein, was based on the consume of NADPH at 480 nm²⁹.

Determination of oxidized and reduced glutathione concentration

To determine oxidized and reduced glutathione concentration, tissue was deproteinized with 2 mol/L perchloric acid, centrifuged for 10 min at 1000 g and supernatant was neutralized with 2 mol/L potassium hydroxide. The reaction medium contained 100 mmol/L phosphate buffer (pH 7.2), 2 mmol/L nicotinamide dinucleotide phosphate acid, 0.2 U/mL glutathione reductase, 70 $\mu\text{mol/L}$ 5,5' dithiobis (2-nitrobenzoic acid). To determine reduced glutathione, the supernatant was neutralized with 2 mol/L potassium hydroxide, to react with 70 $\mu\text{mol/L}$ 5,5' dithiobis (2-nitrobenzoic acid) and read at 420 nm³⁰.

Determination of hydrogen peroxide (H_2O_2)

The assay was based in horseradish peroxidase (HRPO)-mediated oxidation of phenol red by hydrogen peroxide, leading to the

formation of a compound that absorbs at 610 nm. Ventricle slices were incubated for 30 min. at 37°C in phosphate buffer 10 mmol/L (NaCl 140 mmol/L and dextrose 5 mmol/L). The supernatants were transferred to tubes with phenol red 0.28 mmol/L and 8.5 U/mL HRPO. After 5 min incubation, NaOH 1 mol/L was added and it was read at 610 nm. The results were expressed in $\mu\text{moles H}_2\text{O}_2 / \text{g tissue}^{31}$.

Determination of protein concentration

Protein was measured by the method of Lowry³², using bovine serum albumin as standard.

Western Blot (WB) analysis

Tissue homogenization, electrophoresis, and protein transference were performed as described elsewhere^{33;34}. The membranes were processed for immunodetection using rabbit anti-CAT polyclonal antibody, sheep anti-Cu/Zn SOD polyclonal antibody, goat anti-Prx-6 polyclonal antibody primary as (Santa Cruz Biotechnology, Santa Cruz, CA) and rabbit anti-IL-6 polyclonal antibody, mouse anti-TNF- α monoclonal antibody, rabbit anti-Caspase-3 monoclonal antibody primary as (Abcam Inc, CA, USA). The bound primary antibodies were detected using rabbit anti-sheep, rat anti-mouse or goat anti-rabbit horseradish peroxidase-conjugate secondary antibodies and membranes were revealed for chemiluminescence. The generated auto-radiographs were quantitatively analyzed with an image densitometer (Image master VDS CI, Amersham Biosciences Europe, IT). Molecular weights of the bands were determined by reference to a standard molecular weight marker (RPN 800 rainbow full range Bio-Rad, CA, USA). Results from each membrane were normalized through Ponceau red method³⁵.

Histological analyses

From each animal, the cardiac tissue was cut according echocardiographic transverse planes (basal, middle and apical). Tissue was embedded in 10% formalin neutral buffer (pH 7.4), during 48 hours, then embedded in paraffin and cut into semi thin sections 3 to 4 μm thick for microscopy and histological analysis using hematoxylin and eosin staining.

Statistical analysis

Data were expressed as mean \pm SD of n independent experiments. To compare multiple groups, we used two-way ANOVA test (Student-Newman-Keuls Method). The correlation between two variables was analyzed by Pearson's correlation. Tests with $P < 0.05$ were considered statistically significant. Data were analyzed with the SigmaPlot 11.0 program.

Results

Heart rate, infarction size and mortality

The mean HR after sedation during basal echocardiographic evaluation was not significantly different among groups (data not shown). In data observed in the final echocardiogram performed 48 hours post-infarction there was a rise in HR in BMC-treated animals as compared with the non-treated ones; where AMIT HR was increased ($p < 0.01$) compared with AMI group. Infarction area (% of circumference) was not different between AMI and AMIT groups [Table; Figure 1]. Mortality occurred during or immediately after the surgical procedure was around 10% in all groups.

Representative myocardium images – Left ventricular free wall

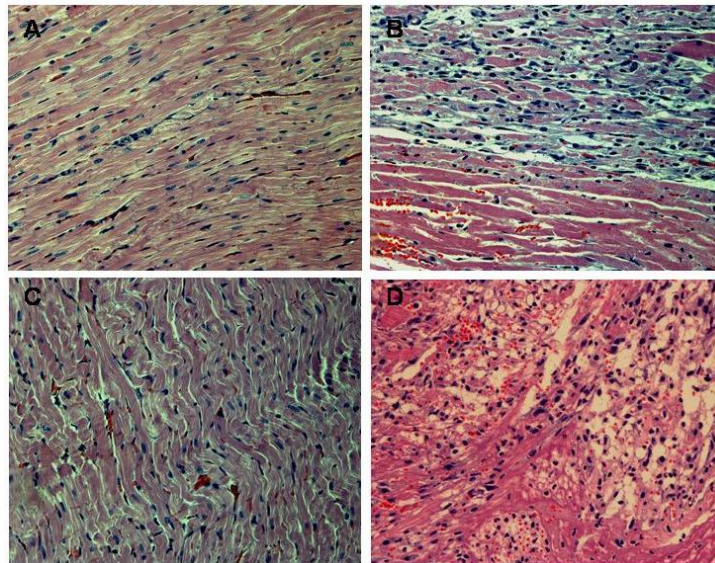


Figure 1 - Representative images of myocardium stained with hematoxylin and eosin (HE) illustrating myocardial transverse diameter showing inflammatory infiltration of infarcted region compared to their respective control groups: (A) Myocardium sample S group (Sham), (B) Myocardium sample AMI group. (C) Non-infarcted myocardium sample with treatment, ST (Sham-treated) group and (D) Infarcted myocardium sample with treatment, AMIT group;

Cardiac dimensions and systolic function

In basal echocardiographic evaluation there was no statistical difference between treated and non-treated groups in all the parameters evaluated (data not shown). In final echocardiographic evaluation assessed 48 hours post-infarction, EF, SD and LVFS were lower in the groups AMI and AMIT, in relation to their respective controls (S and ST, respectively) ($p < 0.001$). At this time point, with the use of BMC was not able to change the profile of these variables in infarcted groups, after 48 hours. Diastolic dimensions and LV mass were not different among groups [Table].

Hemodynamic data

Animals were assessed for LVEDP and LVSP values. AMI and AMIT rats, compared with their controls showed increase in the LVEDP ($p < 0.001$), but without change of LVSP among groups. However, BMC treatment has

not attenuated the rise in LVEDP in the AMIT compared with AMI group [Table].

Organs weight data

The ratio of wet to dry weight in lung and liver of animals were not different in treated and non-treated groups, indicating that there was no lung or liver congestion at this time point. The body weight gain in both treated and non-treated groups was slightly lower than in their respective control groups, however not statistically significant [Table]. Ventricular hypertrophy was observed in infarcted animals compared with the respective controls, AMI vs. S ($p < 0.001$) and AMIT vs. ST ($p = 0.039$) groups. In addition, we observed that the BMC treatment was able to minimize ventricular hypertrophy (AMIT vs. AMI groups) ($p < 0.001$) [Table].

Table – Parameters of cardiac function, hemodynamic profile, oxidative profile and organs weight for each group, with and without BMC treatment.

Characteristic of Animal Groups Parameters	Non-treated		Treated	
	S	AMI	ST	AMIT
Final Echocardiographic Data				
n	11	10	12	14
Heart rate, bpm	243 ± 12	230 ± 22	267 ± 29	270 ± 24 [†]
AHR, %	...	52.8 ± 5.7	...	54.2 ± 4.3
SD, cm	0.339 ± 0.1	0.519 ± 0.04 ^{ψψ}	0.373 ± 0.07	0.519 ± 0.07 ^{**}
DD, cm	0.704 ± 0.1	0.746 ± 0.06	0.744 ± 0.06	0.758 ± 0.07
EF, %	74 ± 7	51 ± 5 ^{ψψ}	73 ± 3	56 ± 10 ^{**}
LVFS, %	53 ± 9	30 ± 4 ^{ψψ}	50 ± 8	31 ± 8 ^{**}
LV Mass, g	0.316 ± 0.08	0.265 ± 0.06	0.282 ± 0.10	0.250 ± 0.08
Hemodynamic data				
n	5	4	10	12
LVEDP, mmHg	6.7 ± 2.3	15 ± 4.7 ^{ψψ}	6.3 ± 1.4	13 ± 2.8 ^{**}
LVSP, mmHg	127.8 ± 16.1	122.1 ± 30.9	114.9 ± 15.0	111.1 ± 15.2
Organs weight data				
n	11	10	10	14
Lung, ratio (wet/dry weight) mg/g	4.75 ± 0.8	4.96 ± 0.3	4.99 ± 0.7	4.85 ± 0.3
Liver, ratio (wet/dry weight) mg/g	3.38 ± 0.2	3.47 ± 0.2	3.54 ± 0.5	3.31 ± 0.3
Body (weight), g	295.2 ± 67.8	265.7 ± 46.4	325.8 ± 47.6	319.9 ± 37.7
Ventricular weight/body weight, mg/g	2.72 ± 0.3	3.40 ± 0.6 ^{ψψ}	2.55 ± 0.3	2.86 ± 0.2 ^{§††}
Antioxidant Enzymes				
n	5	5	5	8
SOD, U/mg protein	5.13 ± 2.0	5.22 ± 1.4	9.34 ± 0.7 [×]	7.2 ± 0.8 [†]
CAT, μmol/mg protein	40.57 ± 8.6	34.06 ± 9.0	31.98 ± 9.6	33.03 ± 9.5
GPx, nmol/mg protein	46.88 ± 9.0	26.32 ± 7.5 ^ψ	36.9 ± 10.7	30 ± 6.5
Oxidative Stress				
n	5	7	6	8
CL, cps/mg protein	5526 ± 1228	6219 ± 969	4169 ± 1035	7392 ± 2223 [*]
H ₂ O ₂ (μmol/mg prot)	32 ± 0.008	22 ± 0.005	116 ± 0.029 ^{xy}	131 ± 0.023 ^{††}
GSH/GSSG, ratio	14.61 ± 3.4	8.21 ± 3.8 ^z	4.7 ± 1.5 ^{xy}	2.1 ± 0.7 [§]

Abbreviations: Akinetic and/or Hypokinetic region, AHR; SD, Systolic Diameter; DD, Diastolic Diameter; EF, Ejection Fraction; Left Ventricular Fractional Shortening, LVFS; Left Ventricular End-Diastolic, LVEDP; and Left Ventricular Systolic Pressures, LVSP; Ventricular weight, Vwt/body weight; Superoxide Dismutase, SOD; Catalase, CAT and Glutathione Peroxidase, GPx activity; Hydrogen Peroxide, H₂O₂ concentration; Chemiluminescence, CL; reduced (GSH) and oxidized glutathione ratio, GSH/GSSG; Data expressed as mean ± SD; p<0.05 was considered statistically significant (Two-way ANOVA test). p<0.001^{ψψ}, p<0.01^ψ, p<0.05^z to S vs. AMI; p<0.001^{**}, p<0.01[†], p<0.05[§] to ST vs. MIT; p<0.001^{xy}, p<0.01[†] to S vs. ST and p<0.001^{††}, p<0.01[†], p<0.005[§] to AMI vs. AMIT;

Flow Cytometry Analysis

To characterize the precursor cells injected, we quantified endothelial precursor cells (KDR⁺/CD34⁺), mesenchymal stem cells (CD44⁺/CD71⁺/CD29⁺) and hematopoietic stem cells (using ISHAGE protocol) in four animals used as cell donors. Endothelial precursor cells corresponded to 1.39% ± 0.87 of the total cells injected, while mesenchymal and hematopoietic fractions corresponded to 0.48% ± 0.09 and 0.48% ± 0.37, respectively.

Antioxidant enzyme activities and expression

Myocardial SOD and CAT activities were not different between AMI compared with S group. On the other hand, treatment with BMC was able to increase SOD activity in both groups ($p < 0.001$). Moreover, infarcted animals that received BMC compared with those that did not receive (AMIT vs. AMI), had increased activity of this enzyme ($p < 0.01$), showing the protective role of BMC against O₂⁻ [Table].

Similar results were found in protein expression of SOD and CAT in cardiac tissue of untreated animals (S and AMI); without difference between groups. However, BMC-treated animals had minor protein expression of SOD ($p < 0.05$) compared to non-treated group [Table; Figure 2A].

GPx activity was depressed in the AMI group in relation to S group ($p < 0.01$). Despite the absence of differences between groups AMI and AMIT, the treatment with BMC was able to maintain the redox balance activity for this antioxidant enzyme in AMIT compared to ST group [Table].

In contrast, CAT protein expression in BMC-treated groups was higher ($p < 0.002$) compared to non-treated groups. In addition, between infarcted groups, cellular therapy was able to increase CAT protein expression

($p < 0.001$). Therefore, the highest CAT protein expression was in AMIT group ($p < 0.001$), showing that although not changing the activity [Table], the treatment was able to increase the CAT protein expression in the presence of an ischemic damage [Figure 2B]. Prx-6 protein expression, responsible by H₂O₂ scavenging, was increased in the AMI group compared to control S ($p < 0.01$) 48 hours post-infarction. Similar result was also found between AMIT compared to control ST group ($p < 0.01$). Nonetheless, the treatment with BMC was not capable of modifying the profile of this protein [Figure 2C].

Oxidation products

Infarction did not cause lipid damage in myocardial tissue at this time point. On the other hand, lipid damage was observed in treated groups, since lipid peroxidation (CL) was increased in AMIT group compared to its control (ST) ($p < 0.01$), although without difference between infarcted groups (AMI and AMIT) [Table].

Hydrogen peroxide (H₂O₂)

H₂O₂ myocardial concentration was not different between AMI and control S groups, while treatment with BMC was capable of modifying their pattern, greatly increasing H₂O₂ concentration in both groups ($p < 0.001$). ST and AMIT groups were not different compared to each other, but the concentration of H₂O₂ was increased in AMIT compared with AMI group ($p < 0.001$), as well as, in ST compared with S group ($p < 0.001$), showing that treated groups had increased production of H₂O₂ [Table]. In addition, a positive correlation between H₂O₂

and caspase-3 ($r=0.803$; $p=0.0001$), was also observed.

GSH/GSSG - reduced to oxidized glutathione ratio

GSH/GSSG ratio was assessed, being depressed in the AMI group compared to control S ($p<0.003$), showing an increase of oxidative stress in this group. We also found a decrease in AMIT as compared with AMI group ($p<0.005$), and between ST and S groups ($p<0.001$). The GSH/GSSG ratio was also

different between ST and AMIT groups, showing that BMC was not capable of maintaining redox balance.

In treated groups, there was an increase in oxidative stress showed by major consumption of glutathione [Table]. In addition, it was found a positive correlation between GSH/GSSG ratio and LVFS ($r=0.639$; $p=0.004$), showing its interaction with cardiac function.

Figure 2 – Graphs illustrating analysis of antioxidant enzymes in cardiac homogenates

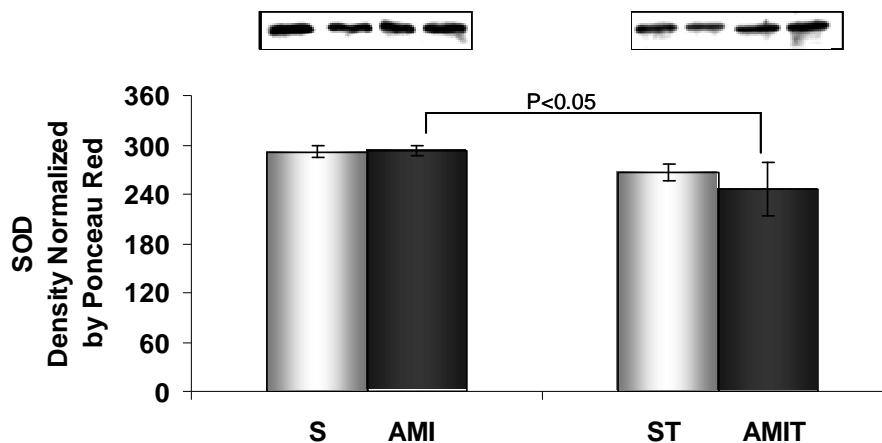


Figure 2 – A) Graph of Western blot analysis in cardiac homogenates using Cu/Zn SOD antibody;

Abbreviations: S, sham; AMI, acute myocardial infarction; ST, sham treated; AMIT, AMI treated; SOD, superoxide dismutase; Note illustrative bands of blots on top part of graphs. $p<0.05$ was considered as statistically significant;

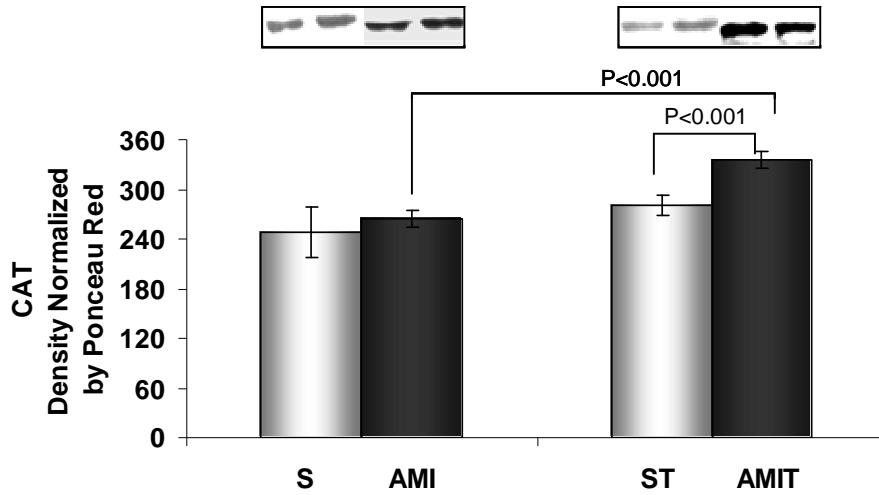


Figure 2 – B) Graph of Western blot analysis in cardiac homogenates using CAT antibody;
Abbreviations: S, sham; AMI, acute myocardial infarction; ST, sham treated; AMIT, AMI treated; CAT, catalase;
 Note illustrative bands of blots on top part of graphs. $p < 0.05$ was considered as statistically significant;

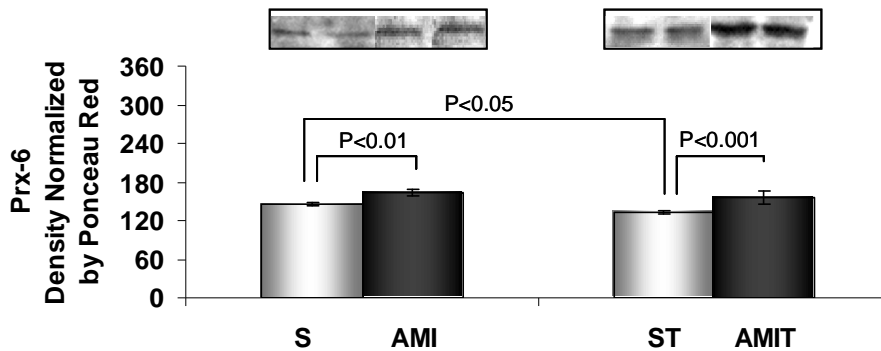


Figure 2 – C) Graph of Western blot analysis in cardiac homogenates using Prx-6 antibody;
Abbreviations: S, sham; AMI, acute myocardial infarction; ST, sham treated; AMIT, AMI treated; Prx-6, peroxiredoxin-6;
 Note illustrative bands of blots on top part of graphs. $p < 0.05$ was considered as statistically significant;

Inflammation and apoptotic markers assessed

TNF- α protein expression was not different between non-treated (AMI vs. S) groups. On the other hand, treatment with BMC was able to reduce this marker expression in infarcted group AMIT, when compared to control AMI ($p < 0.0001$), although the TNF- α expression has been increased in AMIT compared to ST group ($p < 0.05$) [Figure 3A]. Additionally, a moderate correlation between ventricular hypertrophy and TNF- α protein expression was found ($r = 0.732$; $p = 0.001$).

IL-6 expression was increased in AMI compared to S group ($p < 0.001$), as well as, in the AMIT compared to ST group ($p < 0.001$). Nevertheless, the treatment with BMC was capable to reduce this cytokine's expression

($p < 0.0001$). In the infarcted groups, IL-6 expression was minor in AMIT as compared to AMI group ($p < 0.001$) [Figure 3B]. In addition, a moderate correlation between ventricular hypertrophy and IL-6 protein expression ($r = 0.720$; $p = 0.001$) was also observed.

Caspase-3 protein expression was not different between non-treated (AMI vs. S) groups. On the other hand, caspase-3 in AMIT was higher compared to ST group ($p < 0.01$). We observed an increase of caspase-3 in treated groups (ST and AMIT), ($p = 0.0002$), and between non-treated and treated (S vs. ST) groups ($p < 0.01$) and (AMI vs. AMIT) groups ($p < 0.001$), showing that BMC treatment was capable to stimulate apoptotic process [Figure 3C].

Figure 3 – Graphs illustrating analysis of inflammatory and apoptotic markers in cardiac homogenates

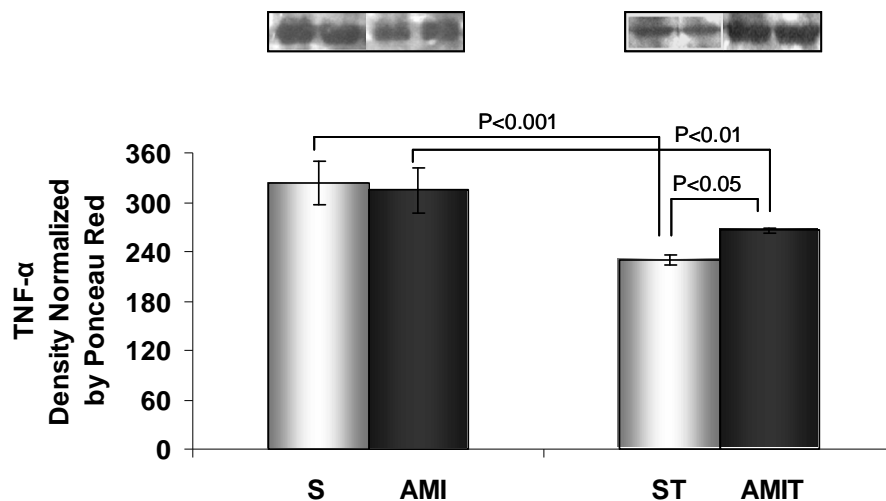


Figure 3 – A) Graph of Western blot analysis in cardiac homogenates using TNF- α antibody; **Abbreviations:** S, sham; AMI, acute myocardial infarction; ST, sham treated; AMIT, AMI treated; TNF- α , tumor necrosis factor- α . Note illustrative bands of blots on top part of graphs. $p < 0.05$ was considered as statistically significant;

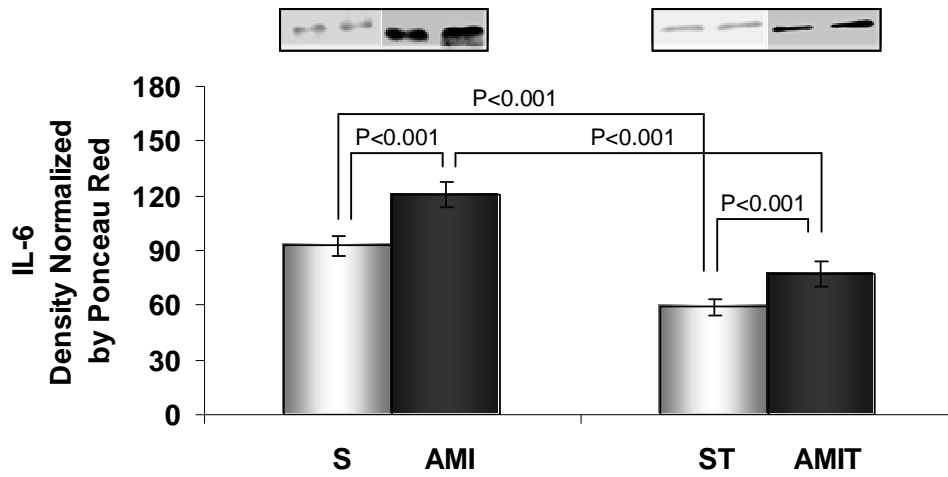


Figure 3 – B) Graph of Western blot analysis in cardiac homogenates using IL-6 antibody;
Abbreviations: S, sham; AMI, acute myocardial infarction; ST, sham treated; AMIT, AMI treated; IL-6, interleukin-6. Note illustrative bands of blots on top part of graphs. $p < 0.05$ was considered as statistically significant;

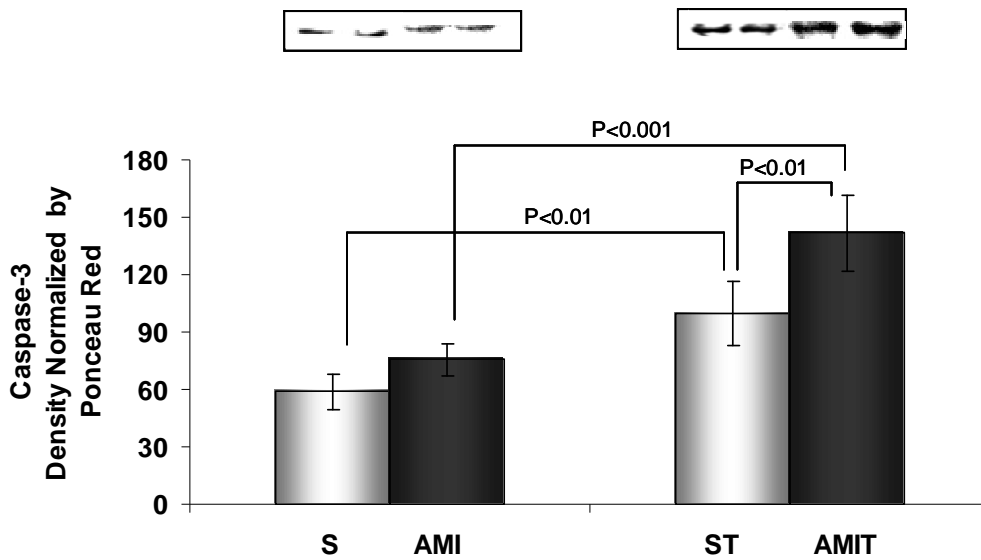


Figure 3 – C) Graph of Western blot analysis in cardiac homogenates using caspase-3 antibody;
Abbreviations: S, sham; AMI, acute myocardial infarction; ST, sham treated; AMIT, AMI treated. Note illustrative bands of blots on top part of graphs. $p < 0.05$ was considered as statistically significant;

Discussion

Early after AMI, cytokines produced locally participate in the recruitment of inflammatory cells, helping the natural process of healing the myocardium and, in this pathologic condition, high concentrations of TNF- α can induce LV dysfunction and cardiac dilation³⁶. In the present study, we were able to show the paracrine effect of BMC treatment in myocardial infarction, assessed 48 hours post-cardiac insult. We observed a decrease in proteic expression of TNF- α and IL-6 in treated groups compared to non-treated, showing that the treatment with BMC was able to interfere in the inflammatory process.

In a study using isolated myocytes and nonmyocytes from non-infarcted myocardium, investigators demonstrated that after myocardial infarction the expression of IL-1 β , IL-6, and TNF- α mRNAs is clearly induced in the nonmyocyte fraction, suggesting possible autocrine and paracrine effect of cardiac nonmyocytes. In a rat model of AMI, membrane bound and soluble TNF- α proteins and mRNA expression significantly increased after 1 and 4 weeks of post-AMI, which correlated positively with LV end diastolic pressure³⁷. This early increase in cytokine levels may reflect the inflammatory response induced by ischemia, and the subsequent rise may reflect healing after myocyte necrosis or a response to heart failure³⁸. The expression of these cytokines can occur simultaneously with early cardiac dysfunction and ventricular compliance changes, suggesting a relation of between these phenomena in a model of ischemia and reperfusion³⁹.

In our study, we saw that there was a decrease in cardiac hypertrophy in BMC-treated group which was directly related to both TNF- α

and IL-6 reduction in its expression. Our findings are in accordance with Franz and colleagues that, recently highlighted amelioration of ventricular remodeling by the use of unfractionated BMC injection compared to other BMC populations and suggested that this effect may be mediated by paracrine secretions of cytokines of transplanted cells, although they only have observed improvement of cardiac hypertrophy, without significant difference in other functional parameters⁴⁰.

The exposure of cells to different concentrations of H₂O₂, increases the endogen levels of cellular TNF- α ⁴¹. In neonatal rat cardiac myocytes, it was found an increase in H₂O₂ resulting in hypertrophy and apoptosis⁴². In contrast to the literature, in our findings, high concentrations of H₂O₂ were not capable of to stimulate TNF- α and/or IL-6 expression in treated groups. In fact, we found an increase of H₂O₂ and consequently increased oxidative stress by GSH/GSSG ratio in treated groups but this was not accompanied by ventricular hypertrophy, at this time point.

A previous study has shown that oxidative stress is one of the mechanisms directly responsible for cardiac dysfunction⁴³. After AMI, oxidative stress develops in both infarcted and non-infarcted myocardium⁴⁴. Moreover, the loss of cardiac function observed by reduced EF, SD and LVFS, and increased of LVEDP in both groups of infarcted animals, can be directly correlated to redox unbalance, as described in other studies^{45;46}.

In a study in patients with HF, it was observed an increase in inflammatory cytokines, TNF- α and IL-6, as well as an increase in the production of hydroxyl radical, post-myocardial infarction. The elevation of both molecules suggests that the interaction between ROS and inflammatory process should

be, probably, related to the progression of LV dysfunction after MI⁴⁷. Our present data indicate that despite of increased oxidative stress, the reduced cytokine expression, use of BMC, probably prevented interaction between ROS and inflammatory process at this time point.

According to Mann and colleagues it is thought that myocardial response to environmental stress is made up of at least two interdependent homeostatic mechanisms: one that allows this tissue to delimit cell injury through upregulation of cytoprotective factors and a second that facilitates tissue repair when and if these cytoprotective responses are insufficient to prevent cell death. However, the mechanisms that are responsible for orchestrating these different stress responses within the myocardium are not known⁴⁸.

Another study using circulating progenitor cells (EPCs), isolated from peripheral blood showed that protein expression of MnSOD, CAT, and GPx was significantly higher in these cells, compared with other cell types. In addition, EPCs due to their higher expression of genes encoding for antioxidative proteins, have low baseline ROS levels and a reduced sensitivity toward ROS-induced cell death⁴⁹.

In our study we assessed expression and activities of antioxidant enzymes, and cellular treatment was capable of increasing expression of SOD and CAT. These effects may be attributed to an increased ROS production, caused by ischemia and consequent O_2^- production⁵⁰.

Previous observations from our group on the profile of H_2O_2 48 hours, post-AMI led us to believe that the transition between compensated and decompensated cardiac function may be influenced by H_2O_2 levels, acting as a signaling molecule activating survival pathways (unpublished data). In our

present study the high H_2O_2 concentrations in treated groups led to an increase of oxidative stress which correlated with increased caspase-3 expression. Apoptotic myocyte cell death precedes cell necrosis, which is a major determinant of infarct size⁵¹. Although cardiac tissue exhibits apoptotic characteristics at this time point, this process may be considered as a survival pathway to the adjacent cells not affected (or barely affected) by ischemia.

Our findings are in agreement with speculations made by Von Harsdorf and colleagues that the induction of apoptosis in cardiomyocytes exposed to ROS in ischemic zones may represent an evolutionarily-conserved protective mechanism that these cells dispose in order to avoid necrosis of other cells and thus risking cardiac function and integrity so early after AMI⁵².

In conclusion, taken together results from the present study revealed that treatment with BMC had a key role in the attenuation of cardiac hypertrophy following infarction, as well as a marked reduction in pro-inflammatory cytokines. It can also be suggested that the apoptotic mechanism observed may lead to decreased necrotic events in remanent myocardium which are more deleterious to the cardiac function, considering that cells in apoptosis cannot signal. In our view, 48 hours post-AMI seems to be an attractive time point to evaluate both paracrine effects exerted by the transplanted cells in the heart tissue as well as the influences imposed upon the cells by the surrounding ischemic environment. Further studies at later time-points are warranted to fully describe potential beneficial effects of BMC therapy in the post-AMI scenario.

Acknowledgements

The authors are grateful to Andreia C. Taffarel (Veterinary Medicine), Gabriela Nicolaidis (Medicine) and Rafael Dall'Alba (Biology), undergraduate students of UFRGS, for their generous contribution. This work was supported by HCPA-FIPE and CNPq grants.

References

1. Grady KL, Dracup K, Kennedy G, Moser DK, Piano M, Stevenson LW, Young JB. Team management of patients with heart failure: A statement for healthcare professionals from The Cardiovascular Nursing Council of the American Heart Association. *Circulation*. 2000;102:2443-2456.
2. Murry CE, Soonpaa MH, Reinecke H, Nakajima H, Nakajima HO, Rubart M, Pasumarthi KB, Virag JI, Bartelmez SH, Poppa V, Bradford G, Dowell JD, Williams DA, Field LJ. Haematopoietic stem cells do not transdifferentiate into cardiac myocytes in myocardial infarcts. *Nature*. 2004;428:664-668.
3. Collins SD, Baffour R, Waksman R. Cell therapy in myocardial infarction. *Cardiovasc Revasc Med*. 2007;8:43-51.
4. Irwin MW, Mak S, Mann DL, Qu R, Penninger JM, Yan A, Dawood F, Wen WH, Shou Z, Liu P. Tissue expression and immunolocalization of tumor necrosis factor-alpha in postinfarction dysfunctional myocardium. *Circulation*. 1999;99:1492-1498.
5. Gwechenberger M, Mendoza LH, Youker KA, Frangogiannis NG, Smith CW, Michael LH, Entman ML. Cardiac myocytes produce interleukin-6 in culture and in viable border zone of reperfused infarctions. *Circulation*. 1999;99:546-551.
6. Hill MF, Singal PK. Antioxidant and oxidative stress changes during heart failure subsequent to myocardial infarction in rats. *Am J Pathol*. 1996;148:291-300.
7. Ungvari Z, Gupte SA, Recchia FA, Batkai S, Pacher P. Role of oxidative-nitrosative stress and downstream pathways in various forms of cardiomyopathy and heart failure. *Curr Vasc Pharmacol*. 2005;3:221-229.
8. Kaur K, Sharma AK, Dhingra S, Singal PK. Interplay of TNF-alpha and IL-10 in regulating oxidative stress in isolated adult cardiac myocytes. *J Mol Cell Cardiol*. 2006;41:1023-1030.
9. Kaul N, Siveski-Iliskovic N, Hill M, Slezak J, Singal PK. Free radicals and the heart. *J Pharmacol Toxicol Methods*. 1993;30:55-67.
10. MacLellan WR, Schneider MD. Death by design. Programmed cell death in cardiovascular biology and disease. *Circ Res*. 1997;81:137-144.
11. Haunstetter A, Izumo S. Apoptosis: basic mechanisms and implications for cardiovascular disease. *Circ Res*. 1998;82:1111-1129.
12. Uemura R, Xu M, Ahmad N, Ashraf M. Bone marrow stem cells prevent left ventricular remodeling of ischemic heart through paracrine signaling. *Circ Res*. 2006;98:1414-1421.
13. Colucci WS. Molecular and cellular mechanisms of myocardial failure. *Am J Cardiol*. 1997;80:15L-25L.

14. Pfeffer MA, Pfeffer JM, Fishbein MC, Fletcher PJ, Spadaro J, Kloner RA, Braunwald E. Myocardial infarct size and ventricular function in rats. *Circ Res.* 1979;44:503-512.
15. Mezey E, Chandross KJ, Harta G, Maki RA, McKercher SR. Turning blood into brain: cells bearing neuronal antigens generated in vivo from bone marrow. *Science.* 2000;290:1779-1782.
16. Perin EC, Dohmann HF, Borojevic R, Silva SA, Sousa AL, Mesquita CT, Rossi MI, Carvalho AC, Dutra HS, Dohmann HJ, Silva GV, Belem L, Vivacqua R, Rangel FO, Esporcatte R, Geng YJ, Vaughn WK, Assad JA, Mesquita ET, Willerson JT. Transendocardial, autologous bone marrow cell transplantation for severe, chronic ischemic heart failure. *Circulation.* 2003;107:2294-2302.
17. Barnett D, Janossy G, Lubenko A, Matutes E, Newland A, Reilly JT. Guideline for the flow cytometric enumeration of CD34+ haematopoietic stem cells. Prepared by the CD34+ haematopoietic stem cell working party. General Haematology Task Force of the British Committee for Standards in Haematology. *Clin Lab Haematol.* 1999;21:301-308.
18. Keymel S, Kalka C, Rassaf T, Yeghiazarians Y, Kelm M, Heiss C. Impaired endothelial progenitor cell function predicts age-dependent carotid intimal thickening. *Basic Res Cardiol.* 2008;103:582-586.
19. da Silva ML, Caplan AI, Nardi NB. In search of the in vivo identity of mesenchymal stem cells. *Stem Cells.* 2008;26:2287-2299.
20. Nozawa E, Kanashiro RM, Murad N, Carvalho AC, Cravo SL, Campos O, Tucci PJ, Moises VA. Performance of two-dimensional Doppler echocardiography for the assessment of infarct size and left ventricular function in rats. *Braz J Med Biol Res.* 2006;39:687-695.
21. Peron AP, Saraiva RM, Antonio EL, Tucci PJ. [Mechanical function is normal in remanent myocardium during the healing period of myocardial infarction--despite congestive heart failure]. *Arq Bras Cardiol.* 2006;86:105-112.
22. Mercier JC, DiSessa TG, Jarmakani JM, Nakanishi T, Hiraishi S, Isabel-Jones J, Friedman WF. Two-dimensional echocardiographic assessment of left ventricular volumes and ejection fraction in children. *Circulation.* 1982;65:962-969.
23. Litwin SE, Katz SE, Morgan JP, Douglas PS. Serial echocardiographic assessment of left ventricular geometry and function after large myocardial infarction in the rat. *Circulation.* 1994;89:345-354.
24. Moises VA, Ferreira RL, Nozawa E, Kanashiro RM, Campos O, Andrade JL, Carvalho AC, Tucci PJ. Structural and functional characteristics of rat hearts with and without myocardial infarct. Initial experience with Doppler echocardiography. *Arq Bras Cardiol.* 2000;75:125-136.
25. Llesuy SF, Milei J, Molina H, Boveris A, Milei S. Comparison of lipid peroxidation and myocardial damage induced by adriamycin and 4'-epiadriamycin in mice. *Tumori.* 1985;71:241-249.
26. Gonzalez FB, Llesuy S, Boveris A. Hydroperoxide-initiated chemiluminescence:

- an assay for oxidative stress in biopsies of heart, liver, and muscle. *Free Radic Biol Med.* 1991;10:93-100.
27. Aebi H. Catalase in vitro. *Methods Enzymol.* 1984;105:121-126.
 28. Marklund, S. Handbook of Methods for Oxygen Radical Research CRC. Pyrogallol autooxidation. 243-247. 1985. Press Boca Raton.
 29. Flohe L, Gunzler WA. Assays of glutathione peroxidase. *Methods Enzymol.* 1984;105:114-121.
 30. Akerboom TP, Sies H. Assay of glutathione, glutathione disulfide, and glutathione mixed disulfides in biological samples. *Methods Enzymol.* 1981;77:373-382.
 31. Pick E, Keisari Y. A simple colorimetric method for the measurement of hydrogen peroxide produced by cells in culture. *J Immunol Methods.* 1980;38:161-170.
 32. Lowry OH, Rosebrough NJ, Farr AL, Randall RJ. Protein measurement with the Folin phenol reagent. *J Biol Chem.* 1951;193:265-275.
 33. Araujo AS, Ribeiro MF, Enzweiler A, Schenkel P, Fernandes TR, Partata WA, Irigoyen MC, Llesuy S, Bello-Klein A. Myocardial antioxidant enzyme activities and concentration and glutathione metabolism in experimental hyperthyroidism. *Mol Cell Endocrinol.* 2006;249:133-139.
 34. Laemmli UK. Cleavage of structural proteins during the assembly of the head of bacteriophage T4. *Nature.* 1970;227:680-685.
 35. Klein D, Kern RM, Sokol RZ. A method for quantification and correction of proteins after transfer to immobilization membranes. *Biochem Mol Biol Int.* 1995;36:59-66.
 36. Bozkurt B, Kribbs SB, Clubb FJ, Jr., Michael LH, Didenko VV, Hornsby PJ, Seta Y, Oral H, Spinale FG, Mann DL. Pathophysiologically relevant concentrations of tumor necrosis factor-alpha promote progressive left ventricular dysfunction and remodeling in rats. *Circulation.* 1998;97:1382-1391.
 37. Kaur K, Sharma AK, Singal PK. Significance of changes in TNF-alpha and IL-10 levels in the progression of heart failure subsequent to myocardial infarction. *Am J Physiol Heart Circ Physiol.* 2006;291:H106-H113.
 38. Yue P, Massie BM, Simpson PC, Long CS. Cytokine expression increases in nonmyocytes from rats with postinfarction heart failure. *Am J Physiol.* 1998;275:H250-H258.
 39. Moro C, Jouan MG, Rakotavao A, Toufektsian MC, Ormezzano O, Nagy N, Tosaki A, de Leiris J, Boucher F. Delayed expression of cytokines after reperfused myocardial infarction: possible trigger for cardiac dysfunction and ventricular remodeling. *Am J Physiol Heart Circ Physiol.* 2007;293:H3014-H3019.
 40. Frantz S, Vallabhapurapu D, Tillmanns J, Brousos N, Wagner H, Henig K, Ertl G, Muller AM, Bauersachs J. Impact of different bone marrow cell preparations on left ventricular remodelling after experimental myocardial infarction 10. *Eur J Heart Fail.* 2008;10:119-124.

41. Kaur K, Sharma AK, Dhingra S, Singal PK. Interplay of TNF-alpha and IL-10 in regulating oxidative stress in isolated adult cardiac myocytes. *J Mol Cell Cardiol.* 2006;41:1023-1030.
42. Kwon SH, Pimentel DR, Remondino A, Sawyer DB, Colucci WS. H₂O₂ regulates cardiac myocyte phenotype via concentration-dependent activation of distinct kinase pathways. *J Mol Cell Cardiol.* 2003;35:615-621.
43. Sabri A, Hughie HH, Lucchesi PA. Regulation of hypertrophic and apoptotic signaling pathways by reactive oxygen species in cardiac myocytes. *Antioxid Redox Signal.* 2003;5:731-740.
44. Lu L, Quinn MT, Sun Y. Oxidative stress in the infarcted heart: role of de novo angiotensin II production. *Biochem Biophys Res Commun.* 2004;325:943-951.
45. Khaper N, Singal PK. Effects of afterload-reducing drugs on pathogenesis of antioxidant changes and congestive heart failure in rats. *J Am Coll Cardiol.* 1997;29:856-861.
46. Sia YT, Parker TG, Liu P, Tsoporis JN, Adam A, Rouleau JL. Improved post-myocardial infarction survival with probucol in rats: effects on left ventricular function, morphology, cardiac oxidative stress and cytokine expression. *J Am Coll Cardiol.* 2002;39:148-156.
47. Valgimigli M, Merli E, Malagutti P, Soukhomovskaia O, Cicchitelli G, Antelli A, Canistro D, Francolini G, Macri G, Mastrorilli F, Paolini M, Ferrari R. Hydroxyl radical generation, levels of tumor necrosis factor-alpha, and progression to heart failure after acute myocardial infarction. *J Am Coll Cardiol.* 2004;43:2000-2008.
48. Mann DL. Stress-activated cytokines and the heart: from adaptation to maladaptation. *Annu Rev Physiol.* 2003;65:81-101.
49. Dernbach E, Urbich C, Brandes RP, Hofmann WK, Zeiher AM, Dimmeler S. Antioxidative stress-associated genes in circulating progenitor cells: evidence for enhanced resistance against oxidative stress. *Blood.* 2004;104:3591-3597.
50. Nordberg J, Arner ES. Reactive oxygen species, antioxidants, and the mammalian thioredoxin system. *Free Radic Biol Med.* 2001;31:1287-1312.
51. Kajstura J, Cheng W, Reiss K, Clark WA, Sonnenblick EH, Krajewski S, Reed JC, Olivetti G, Anversa P. Apoptotic and necrotic myocyte cell deaths are independent contributing variables of infarct size in rats. *Lab Invest.* 1996;74:86-107.
52. von Harsdorf R, Li PF, Dietz R. Signaling pathways in reactive oxygen species-induced cardiomyocyte apoptosis. *Circulation.* 1999;99:2934-2941.

CONCLUSÕES DA TESE

I - O comprometimento da função ventricular precocemente pós-IAM parece se associar com um desequilíbrio do estado redox e este, por sua vez interage com os processos iniciais do fenótipo de remodelamento ventricular.

II - A terapia celular, com células derivadas da medula óssea num modelo experimental de 48 horas pós-IAM foi associada com redução da hipertrofia ventricular e menor secreção de citocinas inflamatórias sugerindo ações parácrinas das células, nesta janela temporal.